InterPore JOURNAL

Special Issue – Iran 2024
Original Research

EXPLORING THE INTER-RELATIONSHIP BETWEEN CLIMATIC CONDITIONS AND HEAT-WATER TRANSFER IN DEFORMABLE CRACKED SURFACE STRATA

Milad Jabbarzadeh, Hamed Sadeghi

Department of Civil Engineering, Sharif University of Technology, Tehran, Iran

Correspondence to:
Hamed Sadeghi,
hsadeghi@sharif.edu

How to Cite:
Jabbarzadeh, M., & Sadeghi, H. (2026). Exploring the Inter-Relationship between Climatic Conditions and Heat-Water Transfer in Deformable Cracked Surface Strata. *InterPore Journal*, 3(1), IPJ010326-2. https://doi.org/10.69631/rk5nyd57

RECEIVED: 11 May 2025
ACCEPTED: 10 Aug 2025
PUBLISHED: 1 Mar. 2026

ABSTRACT

Climate-induced soil desiccation and cracking present escalating challenges to infrastructure stability, necessitating comprehensive investigations of soil-climate interactions. Hence, this study presents a thermo-hydro-mechanical (THM) modeling framework to investigate the response of desiccation-cracked soil to climatic variations. The model was constructed using field observations and statistical analysis and incorporated three years of meteorological data from a susceptible area in Iran. The analysis explored heat conduction, water advection, mechanical deformation, and crack evolution under prolonged environmental conditions. Results revealed that heat flux was highly dependent on temperature gradients and crack geometry. Heat migrates upward from the subsurface when air temperature is lower than soil temperature or during rainfall, conditions typically associated with wet or cold seasons, whereas during warmer periods heat is transferred into the soil. Water flux exhibited strong seasonal variability, with rainfall-driven infiltration through the surface and enhanced evaporation near cracks during dry periods. During rainfall, water flow velocity in soil pores was at least 50 times higher than during warm weather. Moreover, a direct relationship between volumetric strain, temperature, and relative humidity was identified. Crack deformation intensified, and long-term climatic exposure resulted in cumulative shrinkage, increasing on average from 12.5% in the first year to 17.5% in the third year.

KEYWORDS

Arid climate, Cracked soil, Heat conduction, Water advection, Deformation

1. INTRODUCTION

Soil in arid and semi-arid regions undergoes complex thermo-hydro-mechanical (THM) interactions driven by climatic variations. Cracked soils, specifically, demonstrate inherent variability, increased permeability, modified thermal properties, and mechanisms for mechanical stress redistribution. When saturated soil dries, surface tensile stresses develop as pore water pressure drops, and cracking occurs once local tensile stress exceeds the soil's tensile strength. Under repeated wetting-drying cycles, the mechanical compressive-tensile stress state redistributes over time and depth (9, 16, 17, 18, 35). Crack formation depends on several factors, including boundary conditions, soil tensile strength, and moisture loss rate. The cracks, formed due to drying shrinkage, significantly impact heat and moisture transfer, influencing soil strength, and both the magnitude and direction of soil deformation. Such cracks affect the integrity of the soil surface and underlying mass, leading to differential deformation and reducing the serviceability of structures, especially under cyclic wetting-drying conditions. Therefore, understanding the interrelationship between climatic factors and THM processes in cracked soils is essential for assessing infrastructure resilience, predicting land degradation, and improving soil-atmosphere interaction models (29, 30).

According to a report by the United Nations Convention to Combat Desertification (UNCCD), climate change has intensified soil drying globally, with approximately 77.6% of land masses becoming drier over the past three decades (34). This accelerated aridity exacerbates desiccation cracking, leading to enhanced soil degradation and posing significant challenges to agricultural productivity and infrastructure resilience. Adaptation measures, such as wastewater recycling, drought-resistant crops, and reforestation initiatives like Africa's Great Green Wall[a], are essential to mitigate these effects. Otherwise, rising global temperatures, altered precipitation patterns, and increased frequency of extreme weather events contribute to soil desiccation, leading to the formation of new cracks or widening of the existing ones.

Desiccation cracks serve as preferential pathways for water infiltration, evaporation, and heat transfer. This phenomenon can undermine the integrity of infrastructures by altering the hydrological balance within soil structures. A study utilizing advanced 2D imaging and 3D scanning techniques revealed that wetting-drying cycles lead to the formation of subcracks and an increase in total crack length, reflecting soil degradation (41). Furthermore, research on saline soils demonstrated that while soil salinity inhibits cracking, wetting-drying cycles promote it, thereby influencing water evaporation dynamics and geo-structural failures (7, 28). The presence of cracks also alters the thermal properties of soils by modifying their structure and moisture content (17, 39). Cracks can facilitate rapid temperature changes within the soil profile, affecting the thermal regime and potentially leading to further mechanical stresses and deformation.

A numerical model was proposed by Zeng et al. (38) to analyze water evaporation dynamics in cracked soils. Suction-related evaporation mechanisms were incorporated into the model, enabling localized evaporation rates and subsequent water redistribution to be determined. Cracks can also function as capillary barriers by interrupting the continuity of the soil matrix and imposing abrupt changes in suction potential across crack walls. This effect can restrict lateral infiltration and redirect water vertically, altering the moisture distribution and intensifying localized drying or wetting, as demonstrated by Qi et al. (25). A similar study was conducted by Tran et al. (31), in which the HYPROP device[b] was employed in a controlled environment to monitor evaporation and soil temperature, revealing three distinct evaporation stages. It was observed that surface cracks formed exclusively during the constant rate period of evaporation while the soil remained wet.

Additionally, the significant influence of environmental relative humidity (RH) on the behavior of cracked soils has been identified. For instance, an experimental study by Zeng et al. (37) revealed that higher RH

[a] *https://www.unccd.int/our-work/ggwi*

[b] *https://metergroup.com/de/products/hyprop/?srsltid=AfmBOopNpStskc8M8EZ1W6pwjhbWBuIxaLhqEghto5G70Fo54z1WhIjs*

levels decreased evaporation rates and increased water content at crack initiation. A hierarchical cracking process was observed under high RH, in which primary cracks formed first, followed by the propagation of finer sub-cracks. In contrast, lower RH accelerated crack formation, resulting in a longer total crack length.

The varying responses of cracked soil to evaporation and infiltration during hot seasons and rainfall events lead to the development of heterogeneous deformation on the soil surface (27). In this context, a large-scale model test conducted by Zhou et al. (40) investigated the failure mechanisms of cracked soil slopes through whole process, multiphysical monitoring. It was demonstrated that transient saturation around cracks and the formation of preferential flow paths contributed to progressive slope failure, with deformation evolving from shallow movements to overall instability. Additionally, soil creep was captured during evaporation after rainfall, indicating that attention should be paid to slope behavior not only during rainfall but also in the early stages of drying. Similarly, Huang and Azam (12) developed a numerical model to predict weather-induced volumetric changes in cracked expansive clay by integrating bimodal water retention curves, hydraulic conductivity characteristics, and seasonal meteorological data. Their study revealed that crack dynamics play a crucial role in regulating water migration, with open cracks enhancing infiltration during dry periods and sealed cracks limiting moisture penetration in wet years.

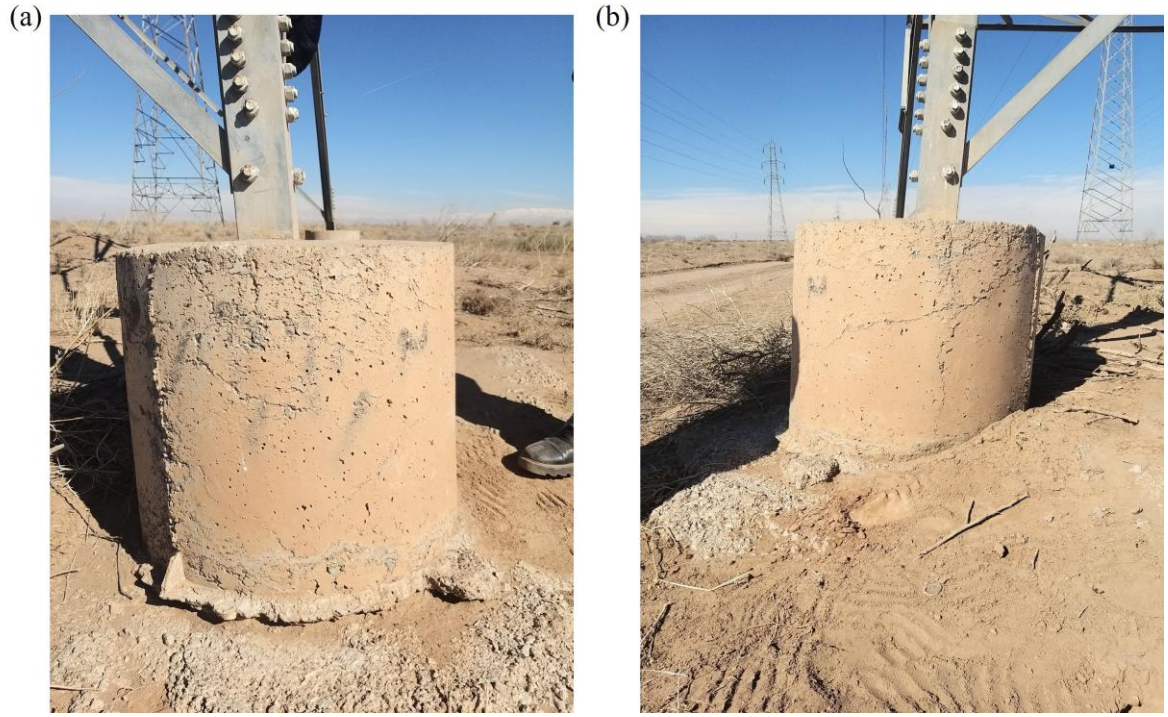

Figure 1: Serviceability issues in power transmission network foundations resulting from crack-induced ground deformation, Qom plain, Iran.

In light of the growing scientific research on the impacts of climate change and existing comprehensive studies on the development of desiccation cracks and their destructive effects on engineering structures (1), it is essential to investigate the thermal, hydraulic, and mechanical behavior of cracked soil in arid climates, while considering the interrelated effects of various factors. Crack networks can progressively develop after the construction of foundations and structures in arid environments, leading to heterogeneous subsidence and differential ground movements that undermine foundation stability and structural safety (1). As illustrated in **Figure 1**, desiccation-induced soil cracking causes heterogeneous ground deformation, leading to foundation serviceability problems in the Qom plain, Iran. In arid regions of Iran such as Kerman, Ardakan (in the Ardakan–Ashkgezar plain), Qom, Eshtehard, and surrounding plains, extensive networks of deep, meter-scale cracks develop after foundation construction and

intensify differential settlement under cyclic climatic wetting and drying (26). For example, field reconnaissance in Kerman revealed pier sinking of up to 8.6 cm/year, buckling of tower members, and masonry wall cracking around substations; similarly, in the Ardakan–Ashkgezar plain near Yazd city, multiple shrinkage cracks repeatedly reach transmission tower piers, exacerbating scour and uneven footing settlements.

Early research on desiccation cracking focused primarily on the mechanics of crack initiation and small-scale propagation under controlled laboratory or limited field settings (3, 22). Although these studies have elucidated fundamental mechanisms of soil cracking and influential factors, they seldom address the consequences once extensive crack networks are established. In arid regions, field-scale cracks, often several meters deep and wide, dramatically alter the soil's thermal and hydraulic regimes, creating complex preferential flow and heat-transfer pathways that amplify and spatially vary volumetric deformation. Despite their critical role in soil–atmosphere interactions and infrastructure performance, these large-scale and heterogeneous effects have been underexplored. Hence, the aim of this study is to apply a THM modeling framework to simulate the long-term response of unsaturated soil with a random crack network under real climatic conditions over a three-year period. The study specifically examines the coupled processes of heat conduction and water advection, and their interaction with atmospheric conditions, leading to mechanical soil deformation. Another aspect of this work is the investigation of how crack widths and areas evolve dynamically over time, with crack narrowing observed under wetting conditions and crack widening under drying conditions, providing new insights into climate-driven deformation mechanisms in arid environments. The insights from this research contribute to a more comprehensive understanding of climate-driven soil THM behavior, offering valuable implications for geotechnical applications, such as infrastructure stability and foundation performance.

2. MATERIALS AND METHODS

2.1. Determination of crack geometric characteristics

Desiccation cracks can exhibit varying dimensions depending on the conditions under investigation. In previous laboratory and numerical studies, crack depth and width have typically been reported in the

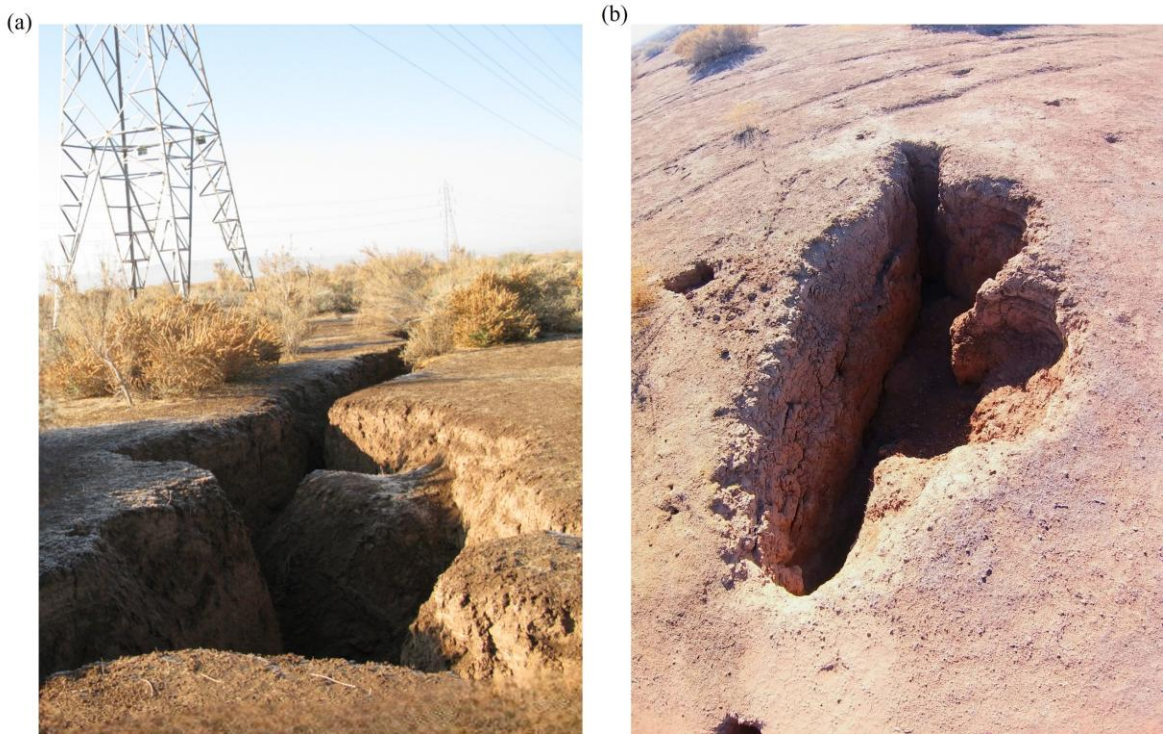

Figure 2: Typical ground surface problems in the vicinity of transmission towers passing subsiding strata, Qom plain, Iran: **(a)** a deep and long crack, and **(b)** a localized deep sinkhole.

 https://doi.org/10.69631/rk5nyd57

range of a few millimeters. However, in large-scale field studies, real cracks can extend several meters. For instance, Gambolati and Teatini (8) documented desiccation cracks with depths ranging from 15 to 20 m. Field observations conducted in the present study also confirmed the presence of deep and wide cracks in the study area.

Qom province of Iran is recognized as a region with an arid climate and has experienced severe land subsidence due to excessive groundwater extraction (14, 21). This arid climate exacerbates the phenomenon, with extreme temperatures contributing to the formation of deep cracks that threaten the stability and integrity of the city's critical infrastructure. **Figure 2** presents images of elongated cracks and localized sinkholes resulting from surface soil desiccation, compounded by groundwater depletion. Although it is difficult to isolate desiccation as the sole mechanism for crack formation under uncontrolled field conditions, the observed cracking patterns in Qom plain are predominantly attributed to desiccation processes, likely intensified by secondary effects such as surface erosion and local soil heterogeneity.

To accurately simulate the study area's conditions, this research focuses on modeling deep and wide cracks. However, determining the exact crack depth is challenging due to various phenomena, such as soil erosion. Therefore, the results of other studies, as summarized by Jabbarzadeh et al. (17), were used to optimize the estimation of crack width and depth, and statistical analyses were conducted to define a representative modeling scenario. Comparing crack sizes or behaviors observed in laboratory and field studies requires careful consideration of differences in boundary conditions, sample size, soil depth, initial stress state, and environmental exposure. These factors strongly influence crack propagation behavior, making direct comparisons of absolute crack dimensions problematic. Following the approach

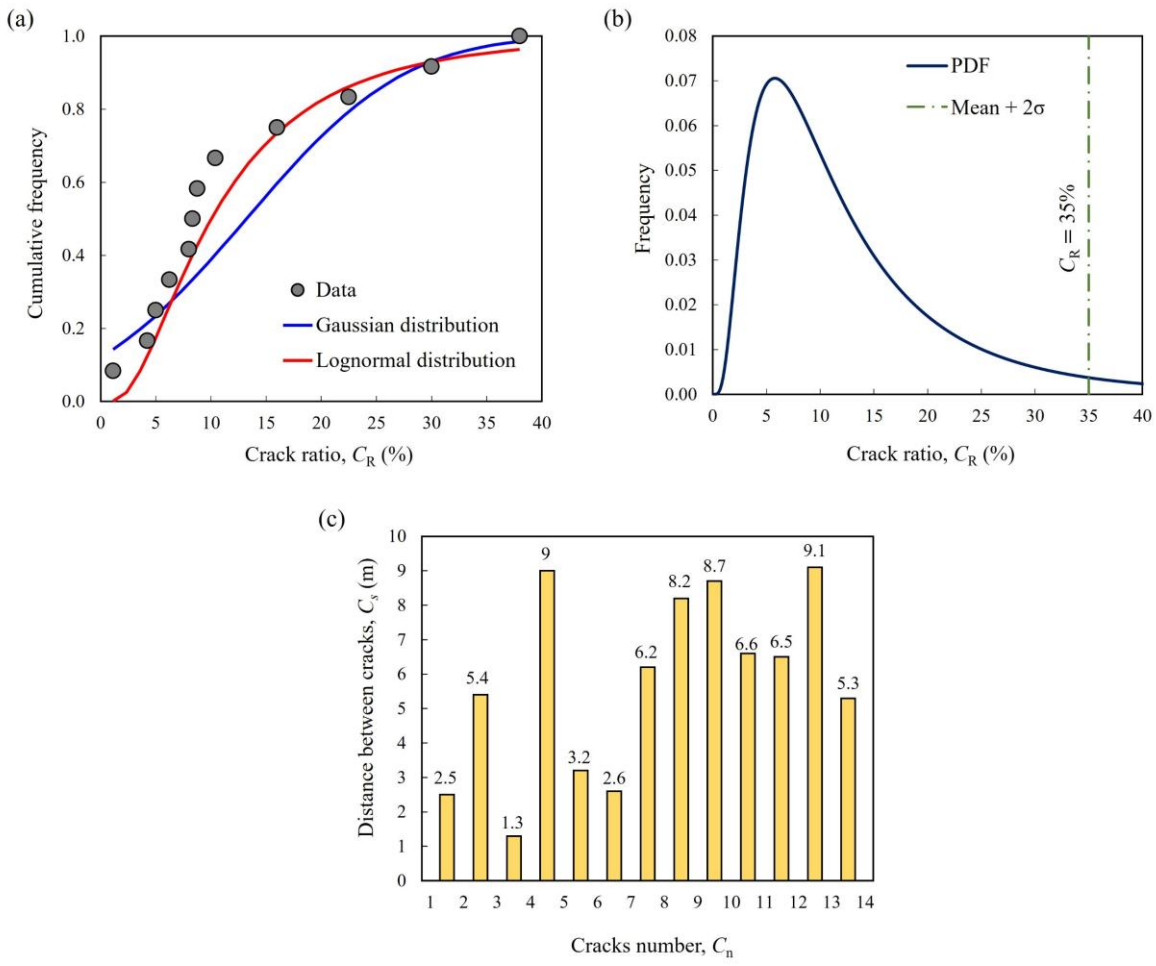

Figure 3: Statistical analysis of crack characteristics: **(a)** cumulative frequency of crack ratio, **(b)** probability distribution function, and **(c)** crack spacing distribution.

 https://doi.org/10.69631/rk5nyd57

of Jabbarzadeh et al. (17), a dimensionless parameter known as the crack ratio (CR), defined as the width-to-depth ratio of the crack, was introduced to leverage a broader range of laboratory, numerical, and field studies while neutralizing the influence of geometric dimensions. A wide spectrum of crack ratio values was gathered from previous studies (refer to Jabbarzadeh et al.; 17), and cumulative frequency and probability distribution functions were plotted in **Figure 3a** and **Figure 3b**. Statistical analysis revealed that the crack ratio follows a log-normal distribution.

Based on field observations, a crack depth of 1 m was selected for the numerical model. To determine the crack width, an appropriate crack ratio was required. According to **Figure 3b**, while the most frequently observed crack ratio in the collected dataset is approximately 5%, more severe field-scale desiccation conditions have been reported in Qom Province (26), and therefore a higher crack ratio was selected. Specifically, a value corresponding to the mean value plus twice the standard deviation (35%) was adopted to represent the upper bound of the observed field data. Given a crack depth (CD) of 1 m and a crack ratio of 35%, the resulting crack width (CW) was calculated as 35 cm.

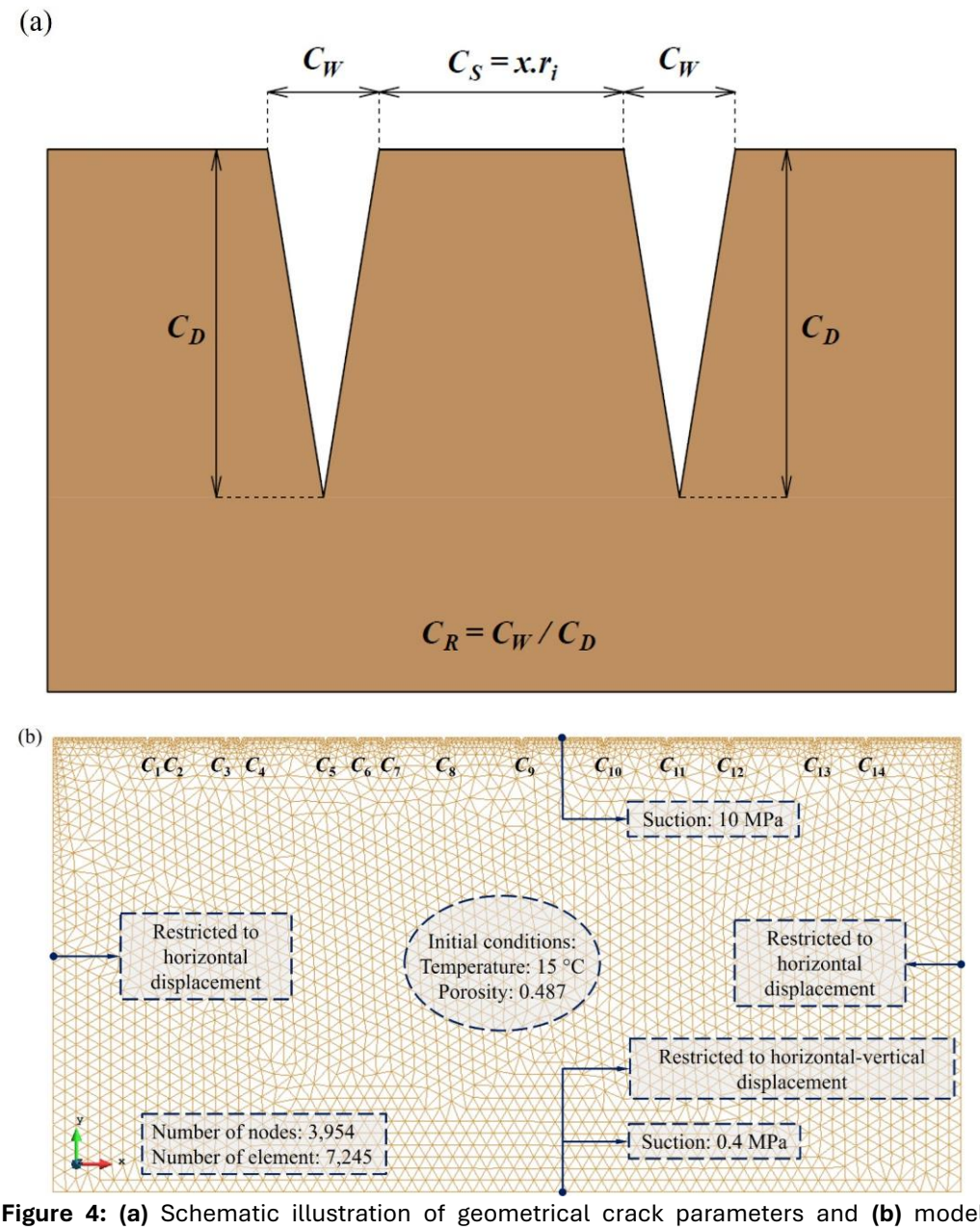

Figure 4: (a) Schematic illustration of geometrical crack parameters and **(b)** model geometry including finite element mesh, initial, and boundary conditions.

 https://doi.org/10.69631/rk5nyd57

In addition to crack geometry, crack spacing (CS) significantly influences the behavior of desiccated soils. Crack networks form randomly in the field, typically influenced by factors such as pre-existing voids, initial microcracks, and heterogeneous bedrock. Accordingly, the spatial distribution of cracks in this study was assumed to be random, with two key constraints: **1)** the minimum crack spacing was set to 1 m, ensuring that cracks were at least as far apart as their depth, and **2)** the maximum spacing was limited to 10 m. Initial numerical analyses indicated that when the crack spacing exceeds 10 m, crack interactions diminish at the midpoint between two cracks. Therefore, 10 m was adopted as the maximum spacing threshold. Therefore, the spatial distribution of cracks generated using a uniform distribution in MATLAB by producing 13 random values between 0.1 and 1, subsequently multiplied by the maximum assumed spacing of 10 m. **Figure 3c** illustrates the corresponding crack spacings, where the shortest distance occurs between the 3rd and 4th cracks (1.3 m), while the largest distance is observed between the 12th and 13th cracks (9.1 m). The geometric parameters and spatial distribution of cracks are schematically depicted in **Figure 4a**. Finally, **Figure 4b** presents the final cracked soil geometry and the finite element meshing of the numerical model, consisting of 7,245 constant-strain triangular elements and 3,954 nodes. The complex field problem is simplified as a two-dimensional model and dimensions were set to 100 m in length and 50 m in depth, accommodating 14 cracks based on the predefined spacing. Additionally, a minimum distance of 10 m was maintained between the lateral boundaries and the first and last cracks to minimize their influence on the results. The mesh at the surface of the model was refined due to the presence of cracks, soil interactions, climatic variations, and the high gradients of moisture and heat exchange between the soil and atmosphere. As shown in **Figure 4b**, the lateral boundaries were restricted in the horizontal direction, while the base boundary was restricted in both horizontal and vertical directions to simulate a fixed support condition. Moreover, the suction values were imposed as Dirichlet boundary conditions on the difference between pore air and pore water pressures at the corresponding boundaries in the model.

2.2. Soil-atmosphere interactions

To model soil-atmosphere interaction, the climatic conditions of Qom were collected over a three-year period from early 2015 to the end of 2017 (13). These meteorological data include temperature, radiation, relative humidity, precipitation, and wind speed, as illustrated in **Figure 5**. These data were applied as Dirichlet boundary conditions to the soil surface and crack walls.

Expansive soils are highly sensitive to moisture variations and are prone to cracking during wetting and drying cycles. In this study, Boom clay was selected as a material for numerical model. Boom clay is well-studied, and its THM properties have been extensively reported (4, 6, 10). The THM parameters used in the numerical model were presented by Sadeghi et al. (27). For the numerical model, an initial soil porosity of 0.487 was assumed, which is consistent with measured values for Boom clay (4, 6, 10).

Field reports from the Qom plain indicate that the groundwater level is deep, approximately 90 m below the ground surface (15). Accordingly, a groundwater depth of 90 m was assumed. Since the model has a 50 m depth, a hydrostatic boundary condition at the base of the model was applied with an initial suction of 0.4 MPa. Given Qom's arid climate, the presence of deep cracks, and the low permeability of the soil, an initial suction of 10 MPa was imposed at the soil surface and along the crack walls. Hence, the suction profile follows a bi-linear distribution extending from the groundwater level to the soil surface. High suction levels are commonly observed in desiccated clayey soils, particularly at the surface where evaporation is dominant. This can be supported using the Kelvin equation, which relates soil suction to temperature and relative humidity (**Eq. 1**):

$$s = -\frac{RT}{v_w \omega_v} \ln(R_H) \tag{1}$$

where R is the universal gas constant ($8.314\ \mathrm{J/(mol \cdot K)}$), T is the absolute temperature (K), v_w is the specific volume of water ($1.0 \times 10^{-3}\ \mathrm{m^3/kg}$), ω_v is the molecular mass of water vapor ($18.016 \times 10^{-3}\ \mathrm{kg/mol}$), and R_H is the relative humidity. On the initial day of the simulation, January 1st, 2015, the recorded air temperature was 15°C (or 288 K), and the relative humidity was 35.5% (i.e., $R_H = 0.355$). Substituting these values into the Kelvin equation yields a suction of approximately 137.76 MPa. Given this result, the

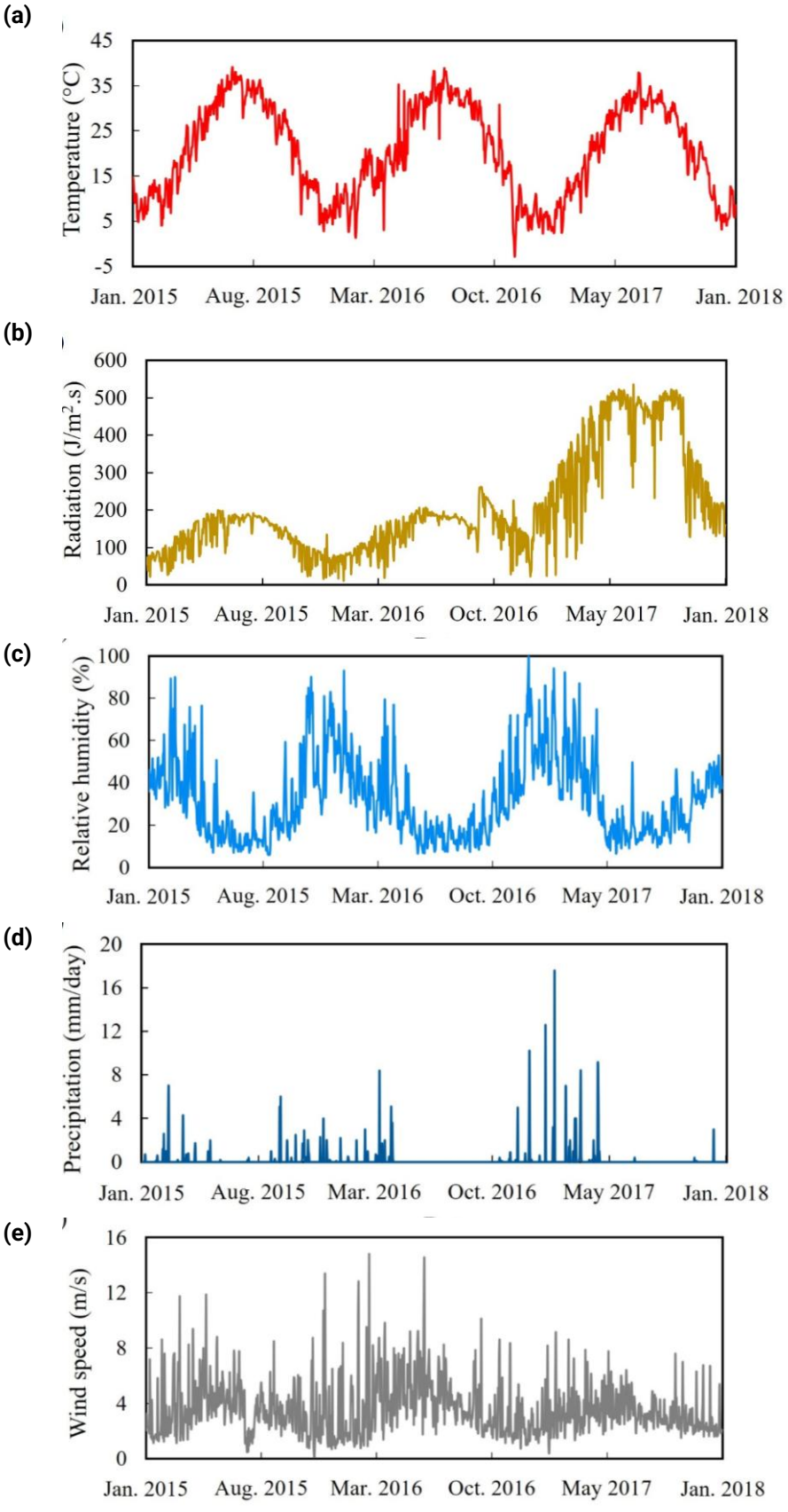

Figure 5: Climatic data of Qom city over a three-year period, including **(a)** temperature, **(b)** radiation, **(c)** relative humidity, **(d)** precipitation, and **(e)** wind speed.

https://doi.org/10.69631/rk5nyd57

assumed initial suction of 10 MPa in the numerical model is a conservative and realistic value for an unsaturated clayey soil that has undergone prolonged drying and cracking. It is expected that under prevailing atmospheric conditions, suction will increase significantly during early simulation steps, justifying the selected initial condition.

According to De Bryune and La Borderie (5), the initial temperature of Boom clay at a depth of 223 m is reported to be 16.6°C. In this study, an initial soil temperature of 15°C was assumed, with temperature variations governed by thermal conduction in response to climatic fluctuations under non-isothermal conditions.

2.3. Description of numerical model framework

The numerical model employed in this study was developed within the finite element framework of CODE_BRIGHT, a well-established THM simulation tool (20, 21). A multiphase and multispecies approach was used, distinguishing solid, liquid, and gas phases while considering water and dry air as the primary species. The formulation of the model relies on fundamental governing principles, including mass, momentum, and energy conservation, which were systematically incorporated to capture the complex interactions within the porous medium.

The model's formulation follows a compositional approach, wherein the mass balance equations account for the independent behavior of solid particles, liquid water, and water vapor in the gaseous phase. The transport mechanisms of these components include advection and diffusion, ensuring an accurate representation of fluid movement through the soil matrix. Energy balance was incorporated under the assumption of thermal equilibrium between phases, allowing the model to capture heat conduction, convective heat transport, and latent heat exchanges. Momentum balance was simplified to stress equilibrium and established by formulating the stress-strain response of the porous medium while incorporating body forces.

For thermal and hydraulic processes, heat transfer was modeled through a conductivity-based approach that accounts for the influence of porosity and saturation using Fourier's law. Fluid flow within the soil was governed by a relative permeability function based on generalized Darcy's law, which considers the impact of soil-water retention behavior and phase interactions. The retention curve was defined using a parameterized formulation of the van Genuchten model (33), capturing the dependency of liquid water content on capillary forces, temperature variations, and air entry values. Additionally, vapor diffusion was incorporated based on Fick's law, accounting for temperature-dependent variations in diffusivity.

The mechanical behavior of the soil was simulated using the Barcelona Expansive Model (BExM) (2), which effectively captures the swelling and shrinkage characteristics of expansive soils. Unlike conventional constitutive models that only account for minor elastic swelling, the BExM framework incorporates microstructural and macrostructural interactions to represent the irreversible volumetric changes caused by changes in suction and mechanical loading. The model defines distinct deformation mechanisms at the micro and macro scales, linking them through a set of coupled yield surfaces and hardening laws. The microstructural response was assumed to follow Terzaghi's effective stress principle, where changes in suction induce a volumetric response similar to that caused by mechanical loading. The macrostructural response was divided into elastic and plastic components, with plastic deformation controlled by a set of yield surfaces corresponding to loading-collapse (LC), suction-induced shrinkage, and suction-induced swelling.

This constitutive model further integrates coupling effects between mechanical and hydraulic processes, where changes in suction influence the soil's volumetric behavior and stress state. The evolution of yield surfaces and hardening mechanisms was defined based on internal variables that track the accumulation of plastic strain in response to wetting-drying and loading-unloading cycles. This approach enables the model to simulate the gradual development of irreversible deformations over multiple climatic cycles (11, 32). For fluid flow, gravity was included in the advective flow component via the hydraulic head term in Darcy's law. In the stress equilibrium equation, gravity was incorporated as a body force vector.

Table 1: Summary of the equations and corresponding variables used in the numerical model.

Equation name	Variable
Balance equations	
Solid mass balance	Porosity, ϕ
Water mass balance	Liquid pressure, P_l
Internal energy	Temperature, T
Stress equilibrium	Displacement, $\dot{u}$
Constitutive equations	
Darcy's law (liquid and gas)	Advective flow, q_l, q_g
Fick's law (vapor)	Non-advective flow, i_g^w
Retention curve (van Genuchten model)	Saturation degree, S_l
Fourier's law	Conductive heat flow, i_c
Mechanical constitutive model (BExM)	Stress-strain, $\sigma - \varepsilon$

By integrating these THM interactions into the computational framework, the model provides a comprehensive tool for analyzing the response of cracked soils to environmental variations. The methodology enables a detailed investigation of heat-water transfer in soil medium, deformation patterns, and pore structure evolution under cyclic climate-induced loading, offering valuable insights into the long-term behavior of geotechnical systems subjected to extreme environmental conditions. The complete set of balance and constitutive equations is presented by Jabbarzadeh et al. (17) and Sadeghi et al. (27). The input material parameters are included in the **Supplementary Material** (available online). The list of equations and related variables are summarized in **Table 1**. Generally, the model assumptions include an initial linear distribution of pore water pressure, a fixed-depth crack geometry, and isotropic, homogeneous soil.

3. RESULTS AND DISCUSSION

3.1. Heat conduction and water advection in cracked soil

Figure 6 illustrates the conductive heat flux within desiccation-cracked soil under three distinct climatic conditions: **i)** the coldest day (day 695) with an air temperature of −1.07 °C (**Fig. 6a**), **ii)** the rainiest day (day 774) with 17.6 mm/day of precipitation (**Fig. 6b**), and **iii)** the warmest day (day 567) reaching 38.74 °C **(Fig. 6c**). As observed, the magnitude and direction of heat conduction depend on both the local geometry (e.g., distance from the crack) and the broader climatic drivers (e.g., temperature, rainfall).

In a porous medium, heat is predominantly transferred via diffusive conduction through both the solid matrix and the pore fluids. In this study, heat transfer by pore fluid advection was neglected, as the relatively low water fluxes in clay under arid conditions result in conduction remaining the dominant mode of heat transfer. When cracks develop, they alter the local pore structure and create preferential pathways that can significantly modify the thermal field. Under colder conditions (**Fig. 6a**) or during rainfall events (**Fig. 6b**), the soil temperature drops relative to subsurface temperatures. Consequently,

heat flows from the warmer subsurface regions toward the cooler near-surface environment. This outward-directed flux arises from Fourier's law, which states that heat conduction occurs along the temperature gradient from higher to lower temperature, consistent with the second law of thermodynamics.

Conversely, on warmer days (**Fig. 6c**), the elevated atmospheric temperature drives heat flow inward, from the hot air into the comparatively cooler soil. This reversal in conduction direction underscores the strong coupling between atmospheric boundary conditions and subsurface thermal behavior in cracked porous media. This observation can be further validated by the experimental study conducted by Zeng et al. (36), which employed infrared thermal imaging to investigate the temperature variations in cracked soil due to evaporation. Under unsaturated soil conditions, water molecules are tightly bound to the soil

matrix, decreasing the evaporation rate. As a result, atmospheric heat energy is transferred to the solid phase of the soil, leading to an increase in the overall temperature of the soil.

The presence of deep cracks significantly affects heat transfer pathways. In intact soils, heat conduction is largely vertical, governed by thermal gradients between the atmosphere and deeper soil layers.

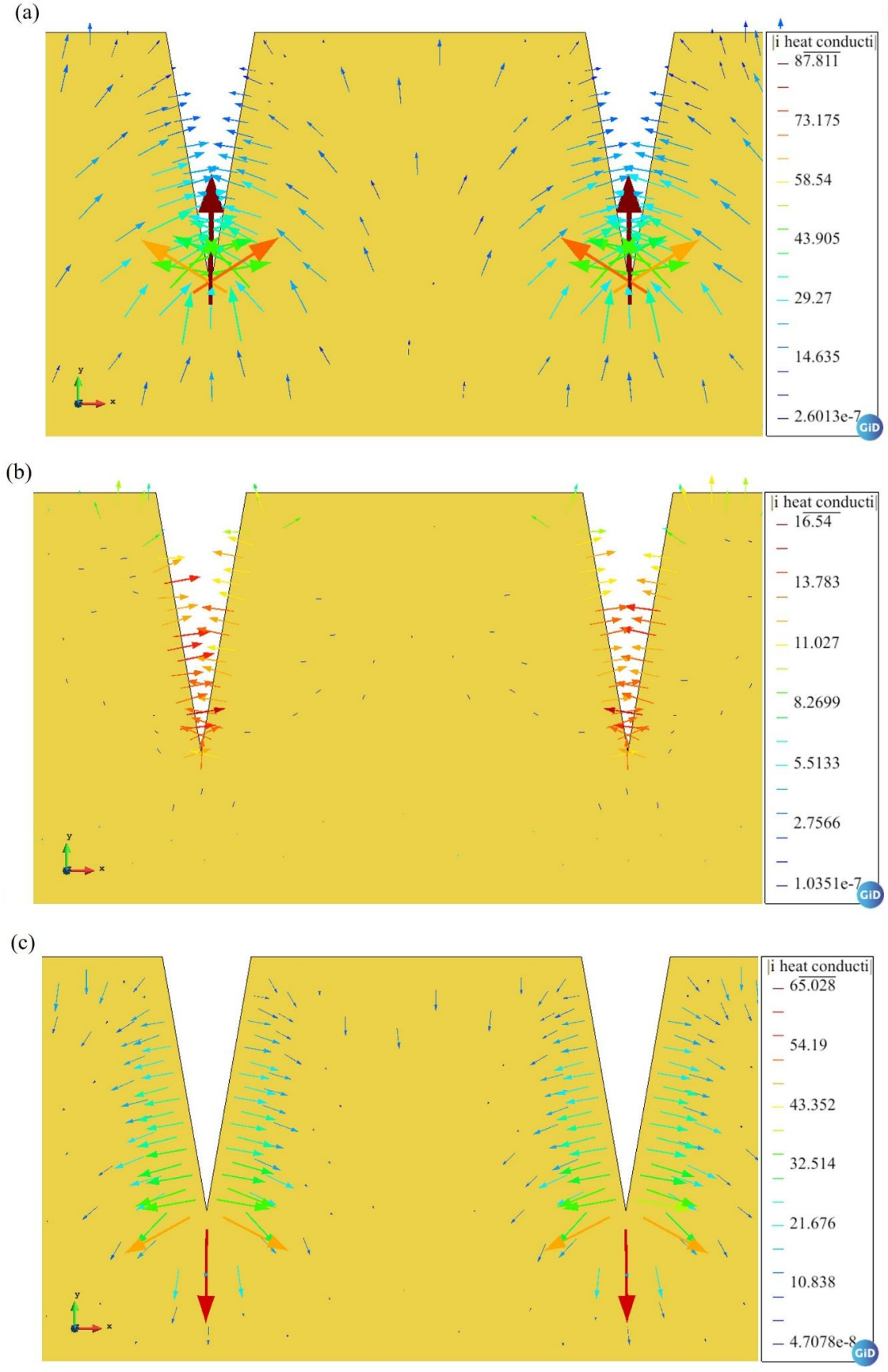

Figure 6: The variability of heat conduction value (W/m·K) and direction under different climate scenarios including **(a)** the lowest air temperature of -1.07°C, **(b)** the highest rainfall of 17.6 mm/day, and **(c)** the highest air temperature of 38.74° C.

 https://doi.org/10.69631/rk5nyd57

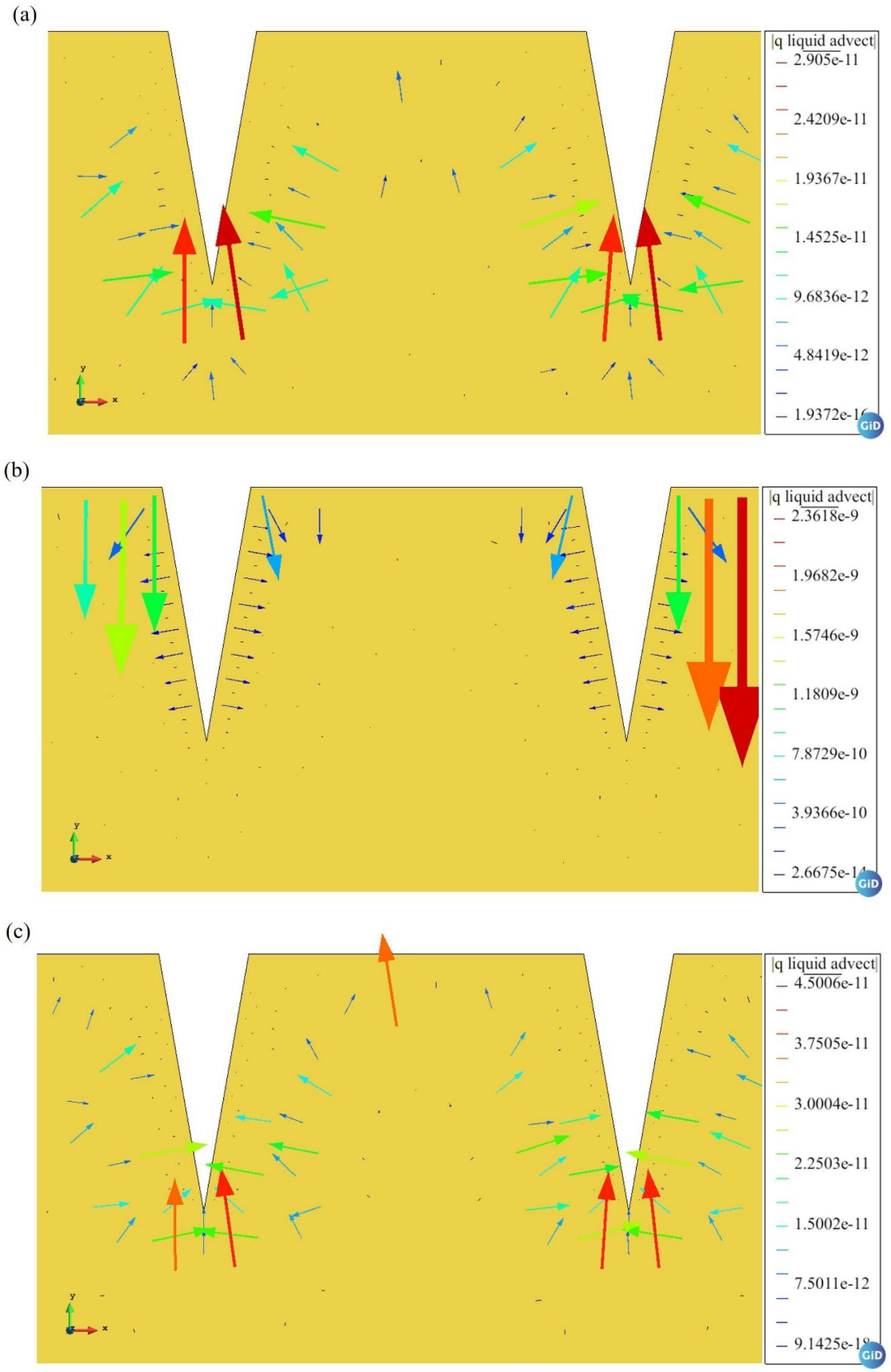

Figure 7: The variability of water advection value (m/s) and direction under different climate scenarios including **(a)** the lowest air temperature of -1.07°C, **(b)** the highest rainfall of 17.6 mm/day, and **(c)** the highest air temperature of 38.74° C.

 https://doi.org/10.69631/rk5nyd57

However, in cracked soils, the crack walls act as additional surfaces through which heat can escape or enter. In practice, these cracks serve as "shortcuts" to the atmosphere, promoting more intense localized fluxes compared to areas without cracks. As shown in **Figure 6a** and **Figure 6c**, crack tips often exhibit heightened heat fluxes.

On rainy days (**Fig. 6b**), water infiltration into the soil pores further complicates heat conduction by modifying local thermal conductivity. Water typically has a higher thermal conductivity than air, so when pores fill with water, heat transfer can be facilitated more efficiently. However, ongoing rainfall also cools the soil surface, often reducing the overall thermal gradient driving conduction. Consequently, the maximum heat flux observed under heavy rainfall (around 16.5 $W\ m^{-1}\ K^{-1}$) is noticeably lower than under extreme hot or cold conditions (65 $W\ m^{-1}\ K^{-1}$ and 88 $W\ m^{-1}\ K^{-1}$, respectively). In addition, as rainwater infiltrates into the soil, it transfers heat from the surrounding soil grains and conveys that energy to deeper layers, potentially redirecting part of the heat flux away from the surface. Meanwhile, the low permeability of clay can delay the percolation of water, allowing heat to be channeled more readily along crack walls rather than through the partially saturated zone beneath the soil surface.

The results confirm that the magnitude of conductive heat flux is highly sensitive to the temperature gradient. Even when water is present in the pore spaces, a strong temperature difference between the soil and the atmosphere dominates heat conduction processes. Cracks introduce heterogeneous pore-scale conditions, altering local porosity, moisture content, and thermal properties. These localized variations can lead to complex patterns of heat flow, including preferential conduction pathways around crack tips or along crack walls. Understanding heat conduction in cracked soils is crucial for predicting temperature distributions, potential evaporation rates, and coupled THM responses, especially in arid and semi-arid regions. Such insights are valuable for infrastructure stability assessments, geothermal studies, and long-term land management strategies.

Figure 7 illustrates the advective flow of water within soil pores under the same three climatic scenarios previously considered for heat conduction: the coldest day (−1.07°C), the rainiest day (17.6 mm/day), and the warmest day (38.74°C). This figure highlights the dynamic interaction between soil moisture and external climatic factors, emphasizing the role of cracks in altering flow patterns and intensifying soil-atmosphere exchanges at greater depths. In general, the direction of water flow is governed by prevailing atmospheric conditions. During rainfall events, water infiltrates into soil pores, driven by gravitational forces, leading to a downward advective flux. Conversely, under dry conditions, increased soil temperatures promote the vaporization of pore water, causing moisture in soil pores to migrate to the atmosphere through evaporation process. The presence of cracks introduces heterogeneities in the porous medium, disrupting the uniformity of flow and creating preferential pathways for water exchange. These pathways facilitate both infiltration and evaporation, occurring not only at the soil surface but also along the crack walls. While the total pressure head distribution governs the general water flux direction in the soil mass, desiccation cracks substantially modify local hydraulic conditions by providing accessible infiltration routes. These features enable rapid and focused infiltration along crack walls and accelerating water movement to deeper soil layers.

Cracks significantly modify the spatial distribution of moisture flux within the soil. The highest advective flow is observed near crack tips, indicating their role in amplifying soil-atmosphere interactions. This phenomenon can be attributed to the increased exposure of deeper soil layers to external climatic influences, leading to enhanced evaporation and moisture loss. Effectively, cracks act as conduits that transport water vapor from subsurface pores to the atmosphere, exacerbating drying processes, particularly in arid conditions. This is consistent with the findings of Tran et al. (31), who discovered that during the early stages of evaporation, the maximum advective flow in the cracked zone exceeds that in the intact zones by over 27%. The findings can be further corroborated by the research conducted by Poulsen et al. (24), which indicated that wind speed and crack width contributed to 49% and 34%, respectively, of the variability in evaporation rates from cracked soils. Their study also revealed that as crack width decreases, evaporation rises, as the relative exposed surface area is greatest at the beginning of crack formation. Poulsen (23) also extended these findings by quantifying that evaporation from cracked soils under moist conditions increased by 60–65% compared to uncracked soils, under similar

wind speed and crack aperture conditions. Notably, evaporation from crack apertures was observed to be up to eight times higher than from an adjacent uncracked soil surface under the same wind conditions.

A comparison between **Figure 7a** and **Figure 7c** reveals a significant contrast in evaporation rates between cold and warm conditions. On cold days, moisture flux is relatively low, with advective flow arrows primarily indicating subsurface movement. The soil surface, which is directly exposed to the atmosphere, exhibits minimal vapor loss, suggesting that evaporation is not a dominant process under these conditions. In contrast, warm weather scenarios (**Fig. 7c**) exhibit a considerably higher evaporation rate, with widespread flow arrows near the crack vicinity and across the soil surface. This observation underscores the role of temperature in accelerating vaporization, where elevated thermal gradients enhance moisture transport from deeper pores to the surface.

Under rainfall conditions (**Fig. 7b**), the infiltration process is distinctly observable, occurring through both the soil surface and the crack walls. However, the infiltration rate is significantly higher at the soil surface compared to the cracks. The advective velocity of water inside soil pores increases sharply during infiltration, in contrast to the relatively low flow rates observed under dry conditions. This phenomenon is attributed to the initial dryness of the soil matrix, where unsaturated soil rapidly absorbs infiltrating water, leading to an abrupt increase in flow velocity. Adsorbed water films on mineral surfaces, resulting from unbalanced negative charges on particle surfaces, together with capillary water held within soil pores in the domain of free water, contribute to the soil's moisture retention capacity and influence water movement under unsaturated conditions. A comparative assessment of the scenarios depicted in **Figure 7** reveals significant differences in water flow velocities. During rainfall, the velocity of water movement within soil pores is at least 80 times greater than that observed under cold conditions and 50 times higher than under warm conditions. These values highlight the strong dependence of advective flow on external climatic drivers.

3.2. Volumetric response of cracked soil to temperature and relative humidity

Figure 8 illustrates the volumetric strain (ε_v) at the soil surface over a three-year period, highlighting its significant correlation with soil temperature. It should be noted that volumetric strain predictions were derived from the combined effects of temperature, radiation, precipitation, wind speed, and relative humidity. In fact, **Figure 8** illustrates the relationship between volumetric strain, influenced by these combined climatic conditions, and temperature. As air temperature rises above soil temperature, heat transfers from the air to the soil, elevating the soil surface temperature. This thermal energy propagates into deeper soil layers via conduction. In unsaturated soils, increased temperature leads to pore water evaporation, increasing negative pore water pressure and causing soil shrinkage, which can result in the formation of new cracks or the expansion of existing ones.

The distribution and spacing of cracks on the soil surface significantly influence the rate and uniformity of volumetric strain, leading to non-uniform and differential deformations. To assess the impact of crack interactions, **Figure 8** compares the $\varepsilon_v - T$ relationship between areas with different crack spacings: 1.3 m (between the 3rd and 4th cracks) and 9.1 m (between the 12th and 13th cracks). The data reveals that volumetric strain increases with rising soil temperature, indicating a decrease in soil pore volume. Conversely, decreasing temperatures slow the shrinkage rate, and if accompanied by increased humidity and water infiltration, can lead to soil swelling. The data indicates a general increasing tendency of volumetric strain with soil temperature, particularly at higher temperatures where data variability diminishes due to the lower likelihood of rainfall events and dominant drying conditions. These linear approximations serve as first-order representations of site-specific trends, providing insight into soil-atmosphere interactions rather than universally applicable predictive models.

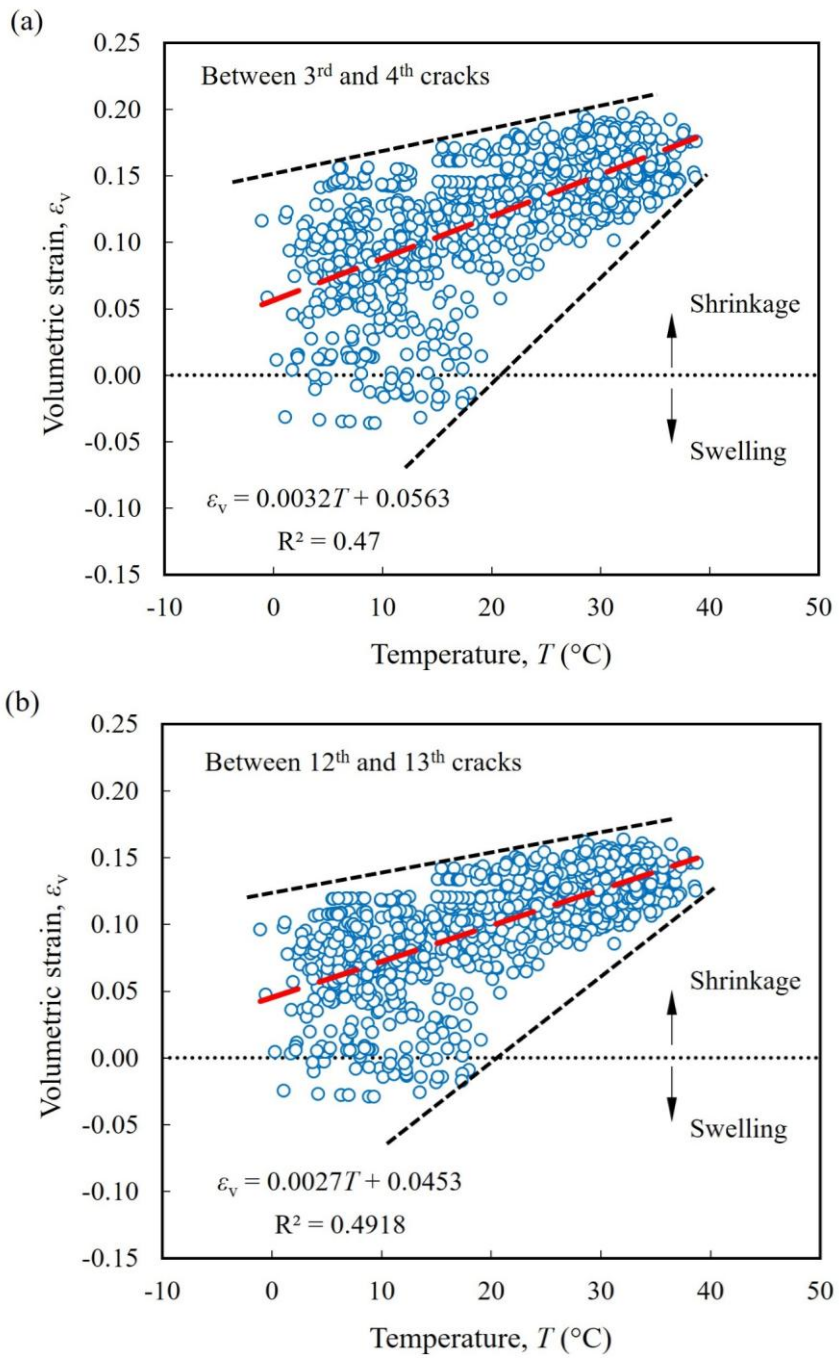

Figure 8: The dependency of soil surface volumetric strain on surface temperature **(a)** between 3rd and 4th cracks, and **(b)** between 12th and 13th cracks, under three years of climate change.

Comparing **Figure 8a** and **Figure 8b** indicates that smaller crack spacing correlates with a higher rate of volumetric strain change in response to soil temperature variations. Specifically, the rate of volumetric strain change at a 1.3-meter crack spacing is approximately 1.2 times greater than at a 9.1-meter spacing. This suggests that closer crack proximity intensifies deformation due to stronger interactions. Additionally, as crack spacing increases, data dispersion in the volumetric strain-temperature plot decreases, enhancing the accuracy of the linear relationship.

Figure 9 presents the seasonal decomposition of volumetric strain data for summer and winter across 2015, 2016, and 2017. This decomposition allows for a more precise analysis of the relationship between temperature variations and soil deformation, reducing uncertainties associated with annual fluctuations. As observed, winter data points exhibit a scattered distribution with significant variability. This dispersion stems from the complex hydromechanical interactions occurring within the porous medium during low temperatures and rainfall events.

 https://doi.org/10.69631/rk5nyd57

Conversely, summer data aligns more closely with a linear trend, yielding higher estimation accuracy. This trend is primarily attributed to the dominant influence of evaporation-driven moisture loss during high temperatures without water infiltration. Soil temperature in the summer varies between 20°C and 40°C, causing volumetric shrinkage of soil pores. The resultant decrease in pore water pressure enhances inter-particle contacts, leading to shrinkage-induced volumetric strain. The observed volumetric strain during summer falls within the range of 10% to 20%, corresponding to the gradual densification of the soil matrix due to persistent drying.

Another observation emerges from comparing **Figure 9a** and **Figure 9d**, where crack spacing effects are evident in both summer and winter. In regions with smaller crack spacing, the rate of volumetric strain variation with temperature is significantly higher compared to areas with wider crack spacing. This can be attributed to the localized concentration of stress and strain within closely spaced cracks, where capillary effects and moisture redistribution occur more intensively. When cracks are closely spaced, the

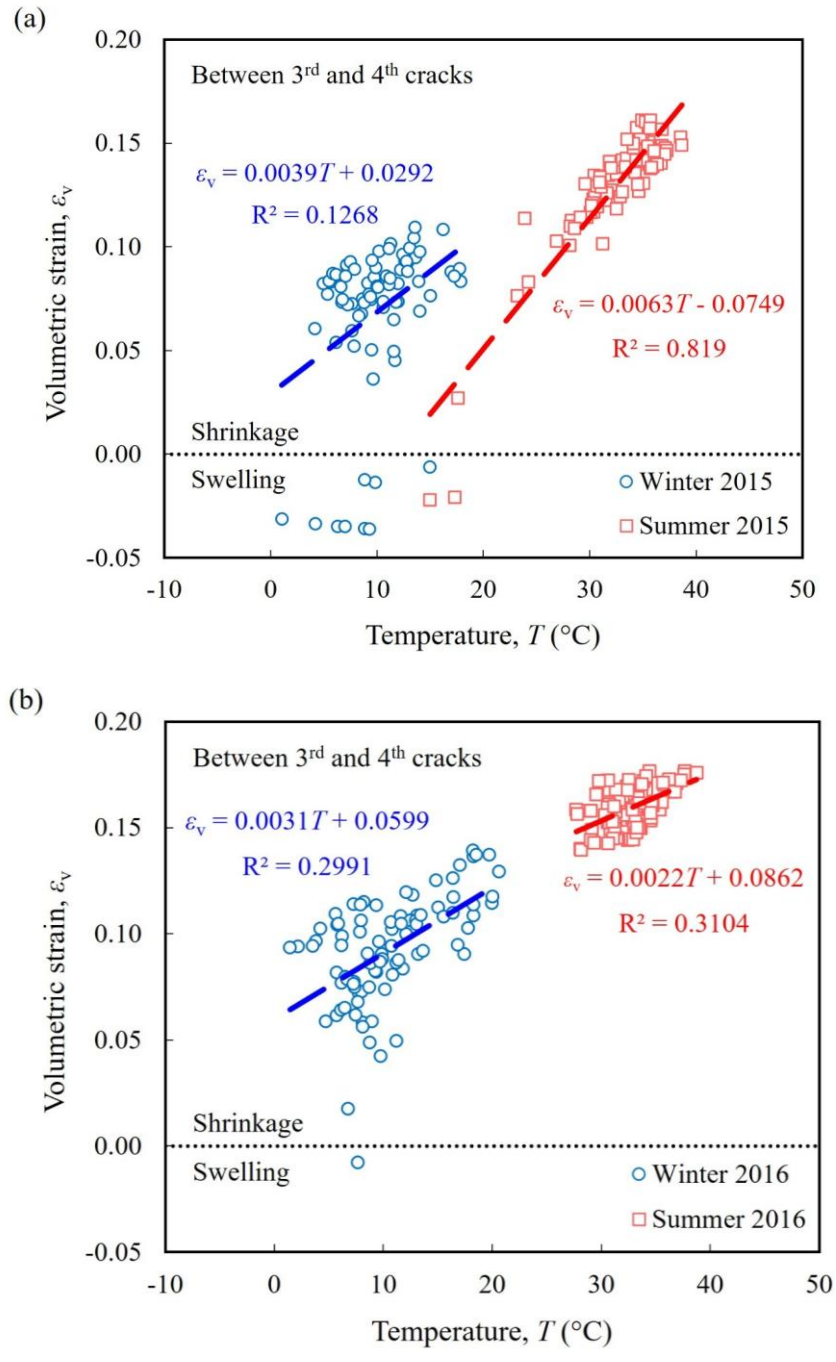

Figure 9: Seasonal variations in cracked soil volumetric strain as a function of soil temperature under environmental loading history.

 https://doi.org/10.69631/rk5nyd57

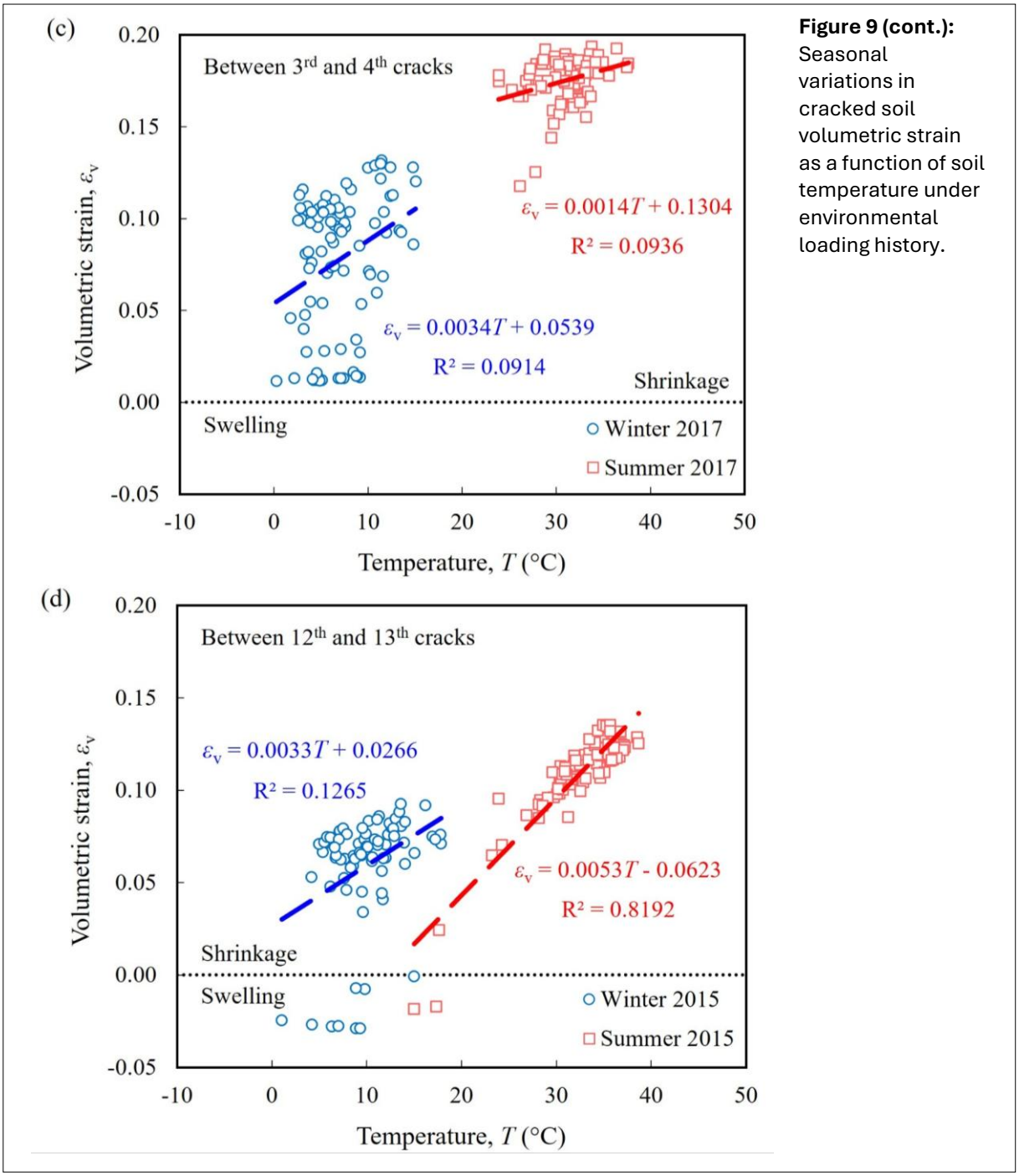

Figure 9 (cont.): Seasonal variations in cracked soil volumetric strain as a function of soil temperature under environmental loading history.

individual capillary suction zones and moisture depletion regions surrounding each crack overlap, intensifying suction gradients and promoting faster moisture loss. This overlap amplifies tensile stress concentrations, leading to higher shrinkage strains under drying conditions. Additionally, closely spaced cracks facilitate more efficient heat transfer through the soil mass, accelerating temperature changes in these zones and further enhancing the thermo-hydro-mechanical response. As shown in **Figure 9a** and **Figure 9d**, this coupled effect results in a steeper relationship between volumetric strain and temperature in soils with smaller crack spacing compared to areas with wider spacing, particularly during warmer periods when evaporation-driven moisture loss dominates soil deformation behavior.

A similar correlation can be established between volumetric strain and relative humidity, as shown in **Figure 10**. Relative humidity is a critical factor influencing the hydro-mechanical behavior of unsaturated soils. The dataset was categorized over a three-year period and analyzed separately for cracks between the 3rd and 4th as well as the 12th and 13th cracks. Relative humidity fluctuations affect soil moisture content through soil-atmosphere interactions. When air relative humidity increases due to rainfall,

condensation, or lower temperatures, soil relative humidity also rises, altering the suction forces within the pore network. Higher RH leads to increased pore water pressure, reducing capillary suction and halting shrinkage-induced volumetric behavior in arid regions. With further RH elevation, pore water pressure becomes sufficient to induce swelling strain, reversing the shrinkage process. This inverse $\mathrm{RH} - \varepsilon_v$ relationship aligns with the temperature correlation discussed earlier. While increased temperature accelerates evaporation and enhances shrinkage, rising RH counteracts this effect by supplying moisture to the soil matrix, promoting swelling. The majority of data points in **Figure 10** fall within the RH range of 10% to 60%, with corresponding volumetric shrinkage strains varying between 5% and 20%.

By comparing **Figure 10a** and **Figure 10b**, a clear trend emerges regarding the impact of crack spacing on soil response to relative humidity changes. In regions with closer crack spacing, RH fluctuations induce larger volumetric strain variations. Conversely, in regions with wider crack spacing, RH variations induce smaller volumetric strain changes, leading to a more uniform response across the soil mass. The

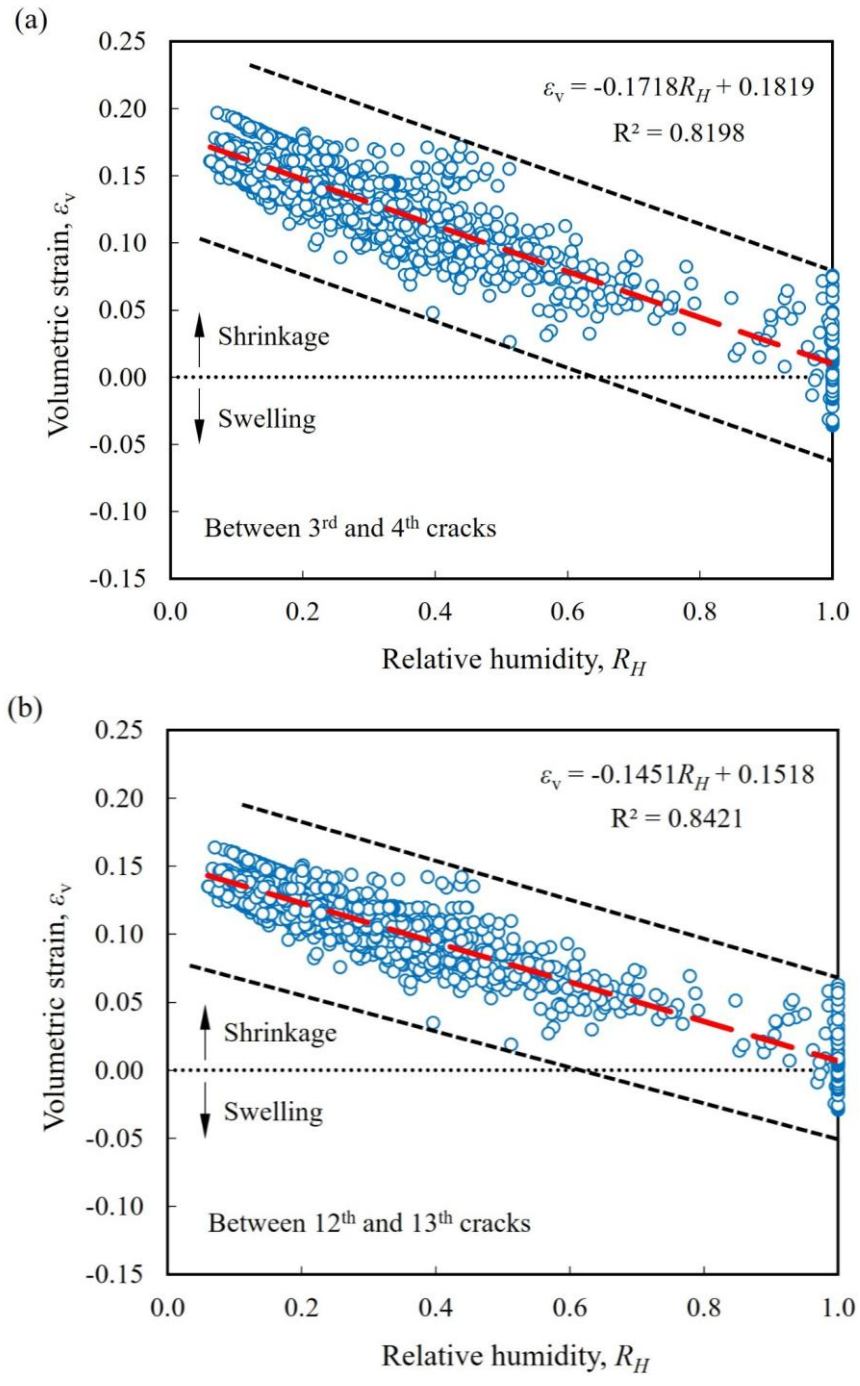

Figure 10: Dependence of soil surface volumetric strain on surface relative humidity: **(a)** between the 3rd and 4th cracks, and **(b)** between the 12th and 13th cracks, over a three-year period.

 https://doi.org/10.69631/rk5nyd57

reduced moisture exchange in these areas results in lower strain gradients, as the redistribution of moisture occurs more gradually. The narrower data dispersion in these regions further supports the notion that increased crack spacing stabilizes soil deformation under varying humidity conditions. Similar to the $T - \varepsilon_v$ relationship, the $RH - \varepsilon_v$ correlation can be approximated using a linear function with reasonable accuracy, as depicted in **Figure 10**. This suggests that relative humidity serves as a reliable predictor for soil deformation behavior, particularly in unsaturated conditions.

As shown in **Figure 10,** volumetric strain exhibits a stronger linear correlation with relative humidity than with temperature. This trend remains consistent even when the data are seasonally decomposed for each of the three consecutive years, as depicted in **Figure 11**. The seasonal approach not only refines the linear approximation but also provides a more nuanced perspective on the shrink-swell cycles of desiccation-cracked soil. By segregating the data into distinct wetting and drying cycles across different seasons, the linear relationship between volumetric strain and RH becomes more pronounced.

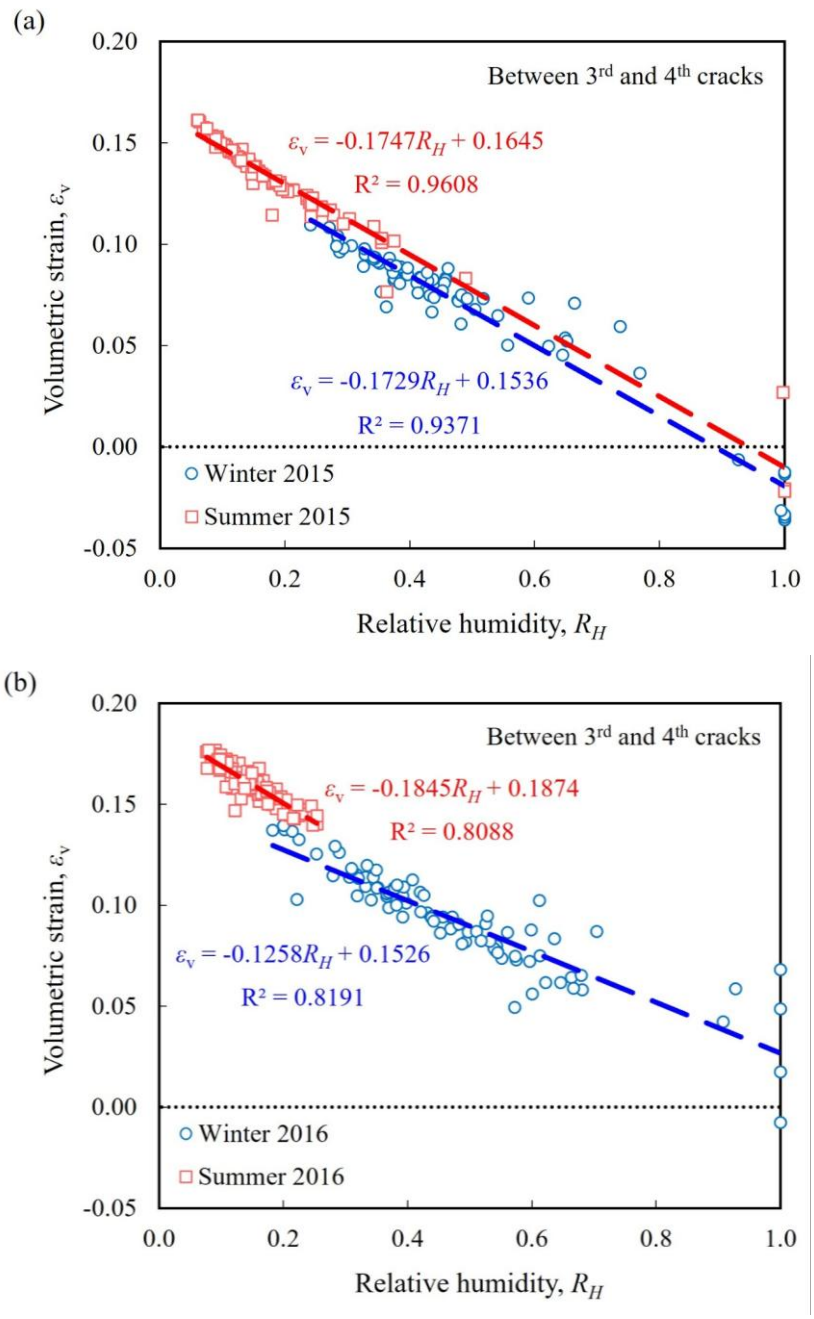

Figure 11: Seasonal variations in volumetric strain of cracked soil with soil relative humidity under environmental loading history.

 https://doi.org/10.69631/rk5nyd57

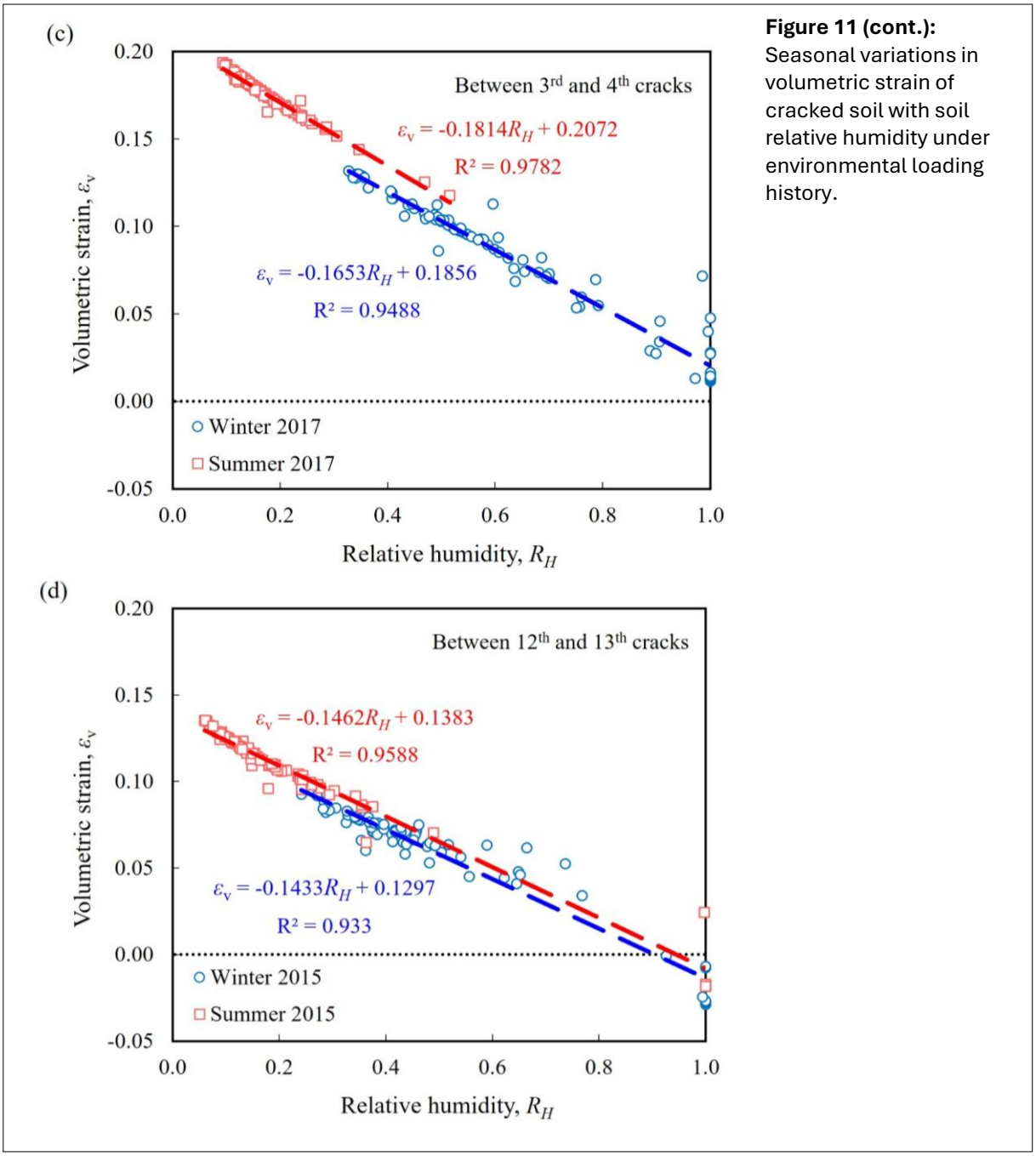

Figure 11 (cont.): Seasonal variations in volumetric strain of cracked soil with soil relative humidity under environmental loading history.

Figure 9 and **Figure 11** collectively indicate that the predominant shrinkage range in the summer of 2015 was approximately 10–15 %, which increased to roughly 14–18 % in 2016, and further to 15–20 % in 2017. This progressive increase underscores how thermo-hydraulic changes in soil medium, driven by evolving climatic conditions, cumulatively exacerbate mechanical deformations over time. As temperatures rise, surface soils, particularly clay-rich horizons, undergo more pronounced drying, a process magnified by desiccation cracks. These cracks effectively expose deeper soil layers to atmospheric conditions, accelerating moisture loss and promoting further shrinkage. From a pore-scale perspective, the interconnected network of cracks and microfractures fosters rapid water vapor migration, lowering the pore water pressure and intensifying the contraction of soil particles. A practical consequence is a net reduction in ground surface elevation over successive years, an observation consistent with the data indicating that volumetric shrinkage does not fully reverse, even during wetter periods.

 https://doi.org/10.69631/rk5nyd57

Another observation from **Figure 11a** is the diminishing occurrence of swelling strains in winter over the study period. For instance, in the winter of 2015, several data points indicated volumetric swelling below the zero-strain line, whereas by 2017, virtually no swelling data appeared. Although precipitation events can still induce partial soil expansion, the ground surface no longer returns to its initial elevation. This trend reflects the irreversible nature of climate-driven soil deformations. The accumulated plastic strains result from repeated cycles of drying and limited rewetting, gradually lowering the soil's capacity to expand to its original volume. This irrecoverable deformation of the soil matrix can be attributed to the rearrangement of particles and potential collapse of microstructures when suction forces are high. Over time, such plastic strains may contribute to subsidence, cracking-induced damage to infrastructure, and other geotechnical challenges.

The temporal trend of swelling strain diminishment is influenced by the initial conditions applied. When a set of driving forces that do not match the initial state (meaning the average steady state of these forces differs from the initial condition) is introduced to the system, it leads to a shift from the original conditions to a new steady state. This transition occurs most rapidly at the beginning and then gradually slows down. In this context, the model simulates a physically meaningful transient adjustment of unsaturated, desiccated cracked soil under long-term atmospheric forcing. The initial suction profile was defined to represent field conditions in Qom, where the groundwater table lies at approximately 90 m depth and the soil surface experiences prolonged desiccation due to minimal rainfall. A non-equilibrium suction distribution was therefore imposed, reflecting realistic field behavior rather than idealized steady-state conditions. The applied atmospheric boundary conditions, based on a three-year climatic dataset, reflect typical arid characteristics, including high temperatures and low humidity. Consequently, the shrinkage-dominated deformation observed in the results arises from the combined effects of **(a)** the transient response to initial non-equilibrium suction conditions, **(b)** continued climatic demand under arid weather, and **(c)** elasto-plastic soil behavior captured by the BExM, which accounts for suction-dependent deformation and its decay over repeated wetting-drying cycles.

During severe drying episodes, capillary forces in pore throats can cause partial collapse of the soil's microstructure. When rewetting occurs, the soil cannot fully recover its original pore configuration, leading to plastic deformation. Meanwhile, development of cracks at the macro scale enhances fluid exchange pathways, facilitating deeper and more rapid drying. At the pore scale, these pathways enable air intrusion and further drying, reinforcing the irreversible nature of volumetric strain. This can also be interpreted by the soil-water retention curve (SWRC). This curve often exhibits hysteresis between drying and wetting cycles. During drying, higher suctions can cause significant shrinkage, whereas subsequent wetting cycles may not fully release these suctions, preserving some degree of contraction and preventing complete rebound.

3.3. Crack deformation due to changes in temperature and relative humidity

As mentioned in Section 2.2, the model incorporates meteorological parameters as inputs, including temperature, wind speed, relative humidity, precipitation, and radiation. Each of these parameters has an impact on the behavior of the crack. In this study, the simultaneous effect of all these parameters was considered. However, under critical climatic conditions, the impact of one parameter can be more significant than others and control the crack's behavior. Therefore, selected days from the three-year period were identified based on the data in **Figure 5**, such that on each day one meteorological parameter reaches its maximum value. The wind speed on the 425th day (14.8 m/s, winter), temperature on the 567th day (38.74 °C, summer), relative humidity on the 727th day (100%, autumn), precipitation on the 774th day (17.6 mm/day, winter), and radiation on the 922nd day (500 J/m2.s, summer) reached their maximum values.

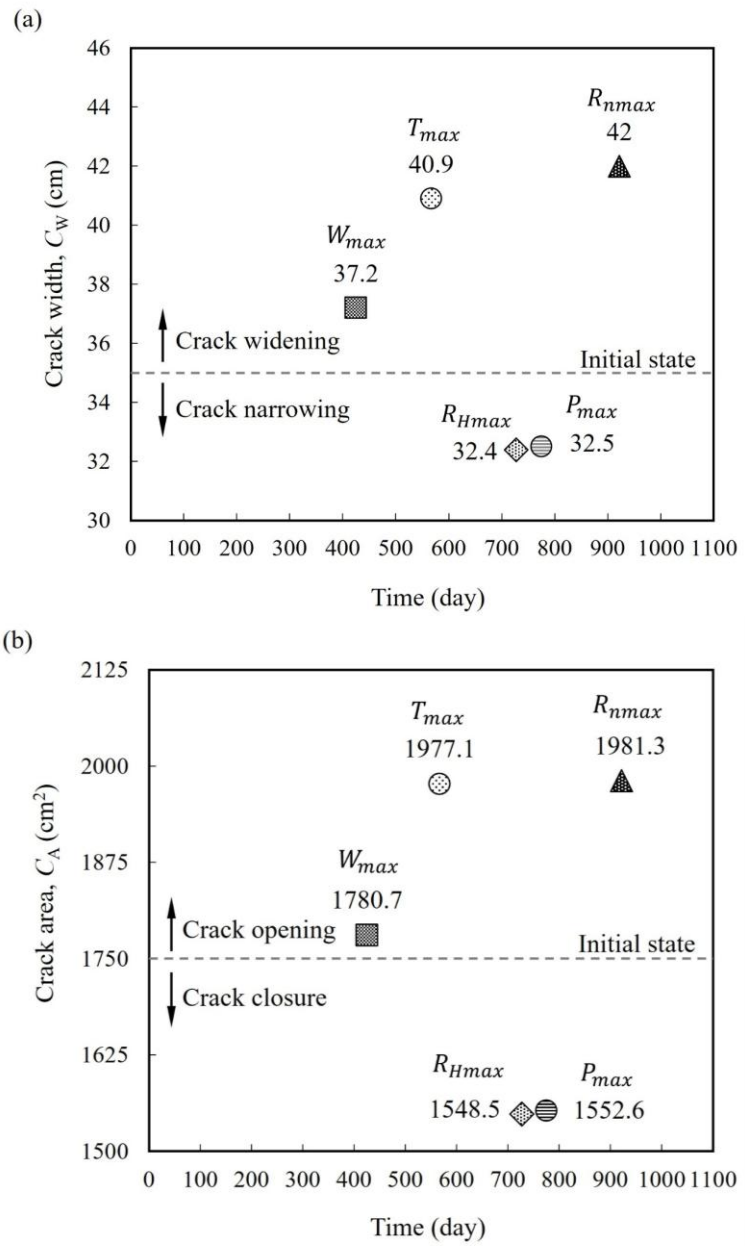

Figure 12: Changes in the **(a)** width and **(b)** area of the 9th crack under extreme climatic conditions.

To assess the effect and intensity of these parameters under critical climatic conditions, the crack width and internal area of the 9th crack on the specified days are presented in **Figure 12**. The results indicate that three factors, namely temperature, wind speed, and radiation, lead to an increase in crack width and area, while the two factors of precipitation and relative humidity result in a decrease in crack width and area. As depicted in **Figure 11a**, the maximum temperature leads to a 5.9 cm increase in crack width. On the day with maximum wind speed and radiation, the crack width increases by 2.2 cm and 7 cm, respectively. Among the factors that contribute to an increase in crack width, radiation has a more significant impact, resulting in a 20% increase. In contrast, relative humidity and precipitation had nearly equal effects in reducing crack width, each contributing to approximately a 7.4% reduction. A similar trend in crack area was observed in **Figure 11b**. The results indicate that maximum wind speed, temperature, and radiation increased the crack area by a maximum of 1.7%, 13%, and 13.2%, respectively. On the other hand, both precipitation and relative humidity reduced the crack area by approximately 11.5%. It should be noted that while the analysis of specific days with maximum values for individual climatic factors provides insight into their relative influence on crack deformation, these factors are not entirely independent in natural conditions. Climatic variables exhibit interdependencies, and the observed effects are influenced by the prevailing values of other parameters on those days. Therefore, the trends presented here reflect indicative tendencies under naturally coupled field conditions.

 https://doi.org/10.69631/rk5nyd57

The geometric behavior of desiccation cracks can be functionally related to both soil surface temperature and relative humidity, which are key drivers in the evolution of pore-scale properties in unsaturated soils. To quantify these relationships, results of the numerical model were used to compute the changes in crack width and internal area at 10-day intervals (i.e., days 0, 10, 20, 30, etc.). **Figure 13a** and **Figure 13b** illustrate that, as temperature increases, both the crack width and the internal crack area also increase. This correlation is attributed to the shrinkage of the soil matrix under elevated temperatures; as the soil dries and shrinks, surface cracks open wider, affecting not only the crack aperture but also the configuration of the crack walls. The increase in the internal area of the crack is thus a combined result of a broader crack opening and deformation of the crack boundaries. These numerical observations align with the results of experimental studies conducted by Zeng et al. (37) and Zhuo et al. (41).

A similar, but even stronger, linear correlation exists between crack geometry and relative humidity, as depicted in **Figure 13c** and **Figure 13d**. With increasing relative humidity, the expansive clay undergoes swelling, which further modifies the crack geometry. Moreover, as noted by Qi et al. (25), the lateral infiltration of crack flow leads to a rapid expansion of the intact soil adjacent to crack walls, which accounts for 80–90% of the crack closure process. This dual dependence on both temperature and

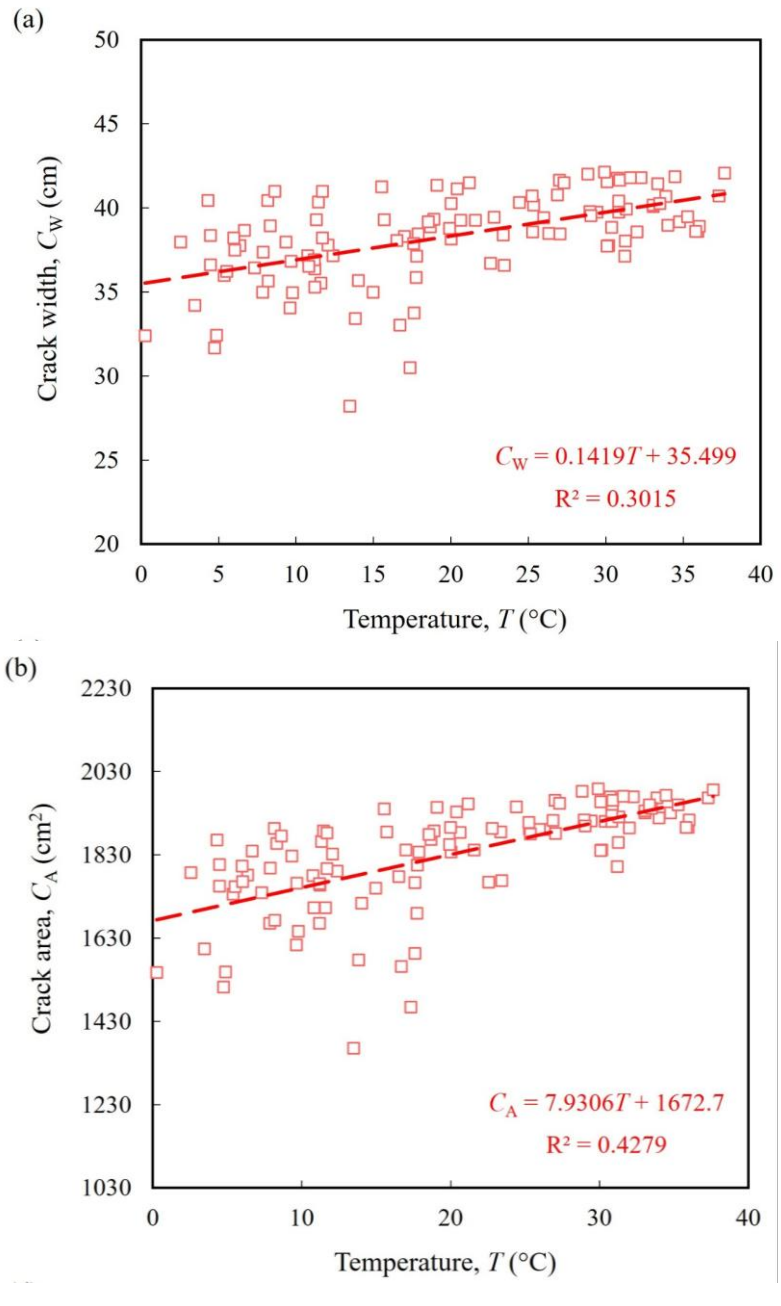

Figure 13: Correlation functions between crack width and area and temperature and relative humidity for the 9th crack.

 https://doi.org/10.69631/rk5nyd57

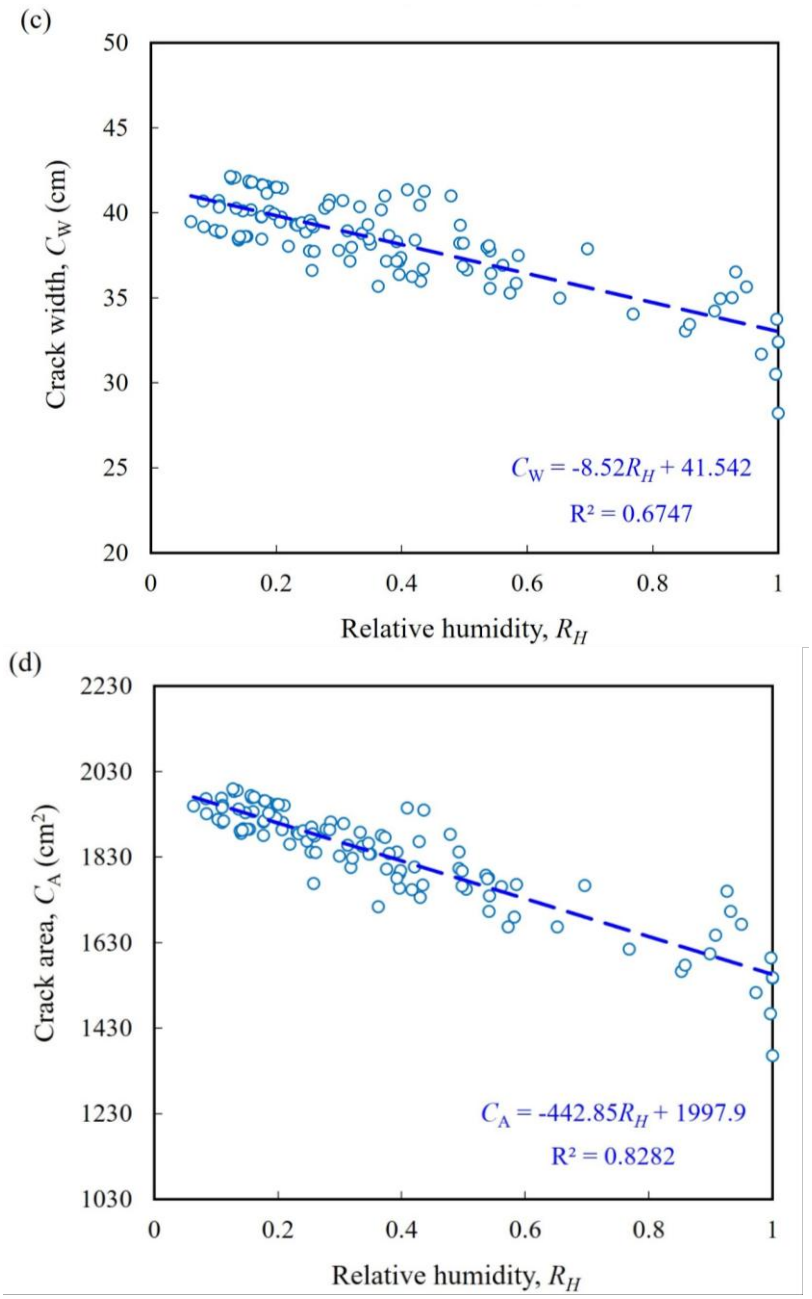

Figure 13 (cont.): Correlation functions between crack width and area and temperature and relative humidity for the 9th crack.

relative humidity is crucial because it reflects the complex interplay between thermal and hydraulic processes at the pore scale. The swelling of clay particles increases the volume within the pore structure, thereby altering both the width and the internal area of the cracks.

Figure 14 extends this analysis by presenting a three-dimensional plot of crack width and internal area as functions of both temperature and relative humidity. A regression plane fitted to these data provides a predictive equation, enabling an initial estimation of crack geometric changes based solely on measurements of soil surface temperature and relative humidity, as shown in **Equations 2** and **3**:

$$C_W = 41.9476 - 0.0133T - 8.8933R_H \quad (2)$$

$$C_A = 1985.7143 + 0.3981T - 431.657R_H \quad (3)$$

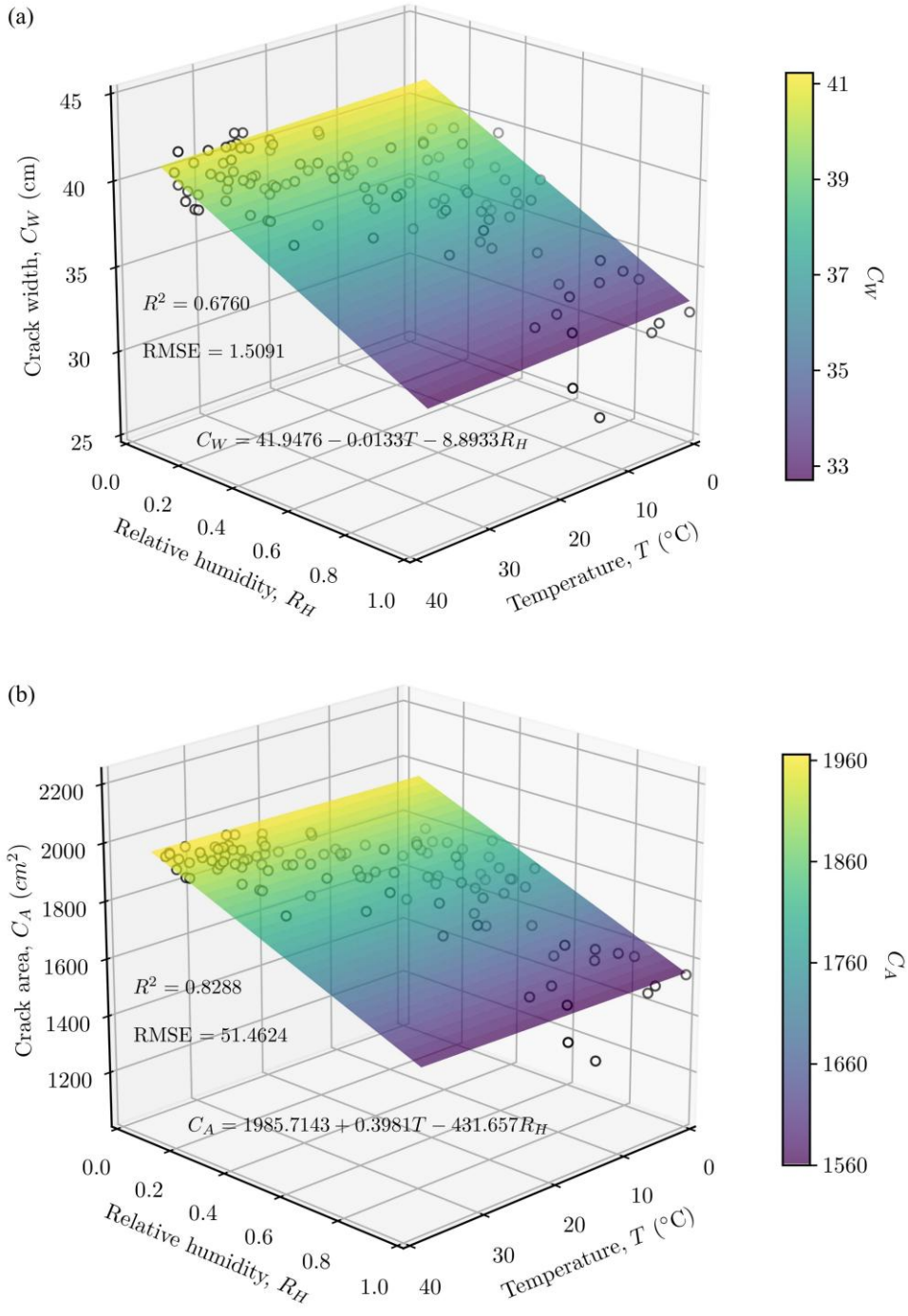

Figure 14: 3D visualization of the correlation between **(a)** crack width and **(b)** crack area with soil surface temperature and relative humidity.

This approach underscores the potential for using easily measurable climatic variables as proxies for more complex pore-scale deformation processes. From a practical standpoint, these findings have significant implications for the prediction and management of soil behavior under climate change. The ability to reliably estimate changes in crack geometry from surface conditions can aid in the assessment of soil stability, subsidence risks, and the long-term performance of geotechnical structures. At the pore scale, these correlations highlight how thermal and moisture variations interact to reshape the soil matrix, influencing both heat-water transport and mechanical strength. Consequently, incorporating these relationships into predictive models can improve the accuracy of simulations for unsaturated soils, providing a more robust basis for engineering decisions in arid and semi-arid regions.

 https://doi.org/10.69631/rk5nyd57

It is important to highlight that the analyses conducted were designed for arid climate conditions and focused on deep, wide cracks in soil with a high potential for volumetric behavior. While the predictive equations are site-specific and may not be applicable in all scenarios, the results from the numerical model are valuable for understanding the thermal, hydraulic, and mechanical responses of cracked soil, as well as its continuous time-dependent behavior and degradation under various wet-dry cycles. Therefore, they are highly relevant for real-world conditions. The regression planes serve as practical first-approximation tools to illustrate the general tendencies of crack deformation under coupled climatic factors for this site-specific case. Their primary value lies in offering qualitative insights into thermo-hydro-mechanical processes in cracked soils, rather than in providing predictive models for crack dimensions.

4. CONCLUSIONS

The well-established thermo-hydro-mechanical formulations were used within a finite element method. A combination of three-year field climate data, elasto-plastic constitutive models, and statistically derived crack geometries were employed to address a complex, large-scale soil-atmosphere interaction problem in soil characterized by randomly distributed wide and deep cracks, a topic that has largely been overlooked in previous numerical investigations. Using three years of meteorological data from Qom, Iran, the study was focused on exploring heat conduction, water advection, mechanical deformation, and crack evolution under prolonged climatic exposure. The key results of this study can be summarized as follows:

Heat flux is highly dependent on temperature gradients and crack geometry. During colder conditions or rainfall events, heat migrates from the subsurface to the surface, while in warmer conditions, heat is transferred into and stored within the soil. Cracks act as preferential pathways for heat transfer, facilitating enhanced fluxes along their walls. Maximum heat flux values were observed under extreme cold (88 W m^{-1} K^{-1}) and hot conditions (65 W m^{-1} K^{-1}), whereas rainfall events significantly reduced heat flux (16.5 W m^{-1} K^{-1}), highlighting the influence of moisture on thermal conductivity.

Water flux patterns demonstrated strong seasonal variations. During rainfall events, water infiltration occurs primarily through the soil surface, with cracks playing a secondary role. In contrast, under dry conditions, moisture migrates toward the atmosphere through evaporation, which is significantly higher near cracks. The study found that water flow velocity during rainfall is at least 80 times higher than in cold conditions and 50 times higher than in warm conditions.

Mechanical deformation analyses showed a clear relationship between volumetric strain, temperature, and relative humidity. Higher temperatures induced soil shrinkage and lower temperatures reduced the shrinkage rate. The presence of cracks intensified deformation, as smaller crack spacing led to greater changes in volumetric strain. Additionally, relative humidity played a crucial role in modifying hydro-mechanical behavior, with higher humidity levels increasing pore water pressure and promoting swelling, counteracting shrinkage effects.

Progressive climate-driven soil deformations result in irreversible subsidence over time. Shrinkage strains increased from 10–15% in 2015 to 15–20% in 2017, indicating cumulative mechanical deterioration under repeated climatic cycles. The interconnected network of cracks facilitates rapid vapor migration, leading to lower pore water pressure and further soil shrinkage. This contributes to a long-term net reduction in ground surface elevation, with volumetric shrinkage effects persisting despite periodic rainfall events.

STATEMENTS AND DECLARATIONS

Supplementary Material

The thermo-hydro-mechanical material parameters which were used in the numerical model are summarized in the Supplementary Material, which is available online here.

Acknowledgements
This work is based upon research funded by Iran National Science Foundation (INSF) under project No. 4035488.

Author Contributions
M. Jabbarzadeh: Conceptualization, Methodology, Investigation, Software, Formal analysis, Validation, Visualization, Writing - Original Draft. **H. Sadeghi:** Conceptualization, Methodology, Supervision, Writing - Review & Editing.

Conflicts of Interest
The authors declare that they have no known competing financial interests or personal relationships that could have appeared to influence the work reported in this paper.

Data, Code & Protocol Availability
The data that support the findings of this study are available from the corresponding author upon reasonable request.

Funding Received
This work is based upon research funded by Iran National Science Foundation (INSF) under project No. 4035488.

ORCID IDs
Milad Jabbarzadeh https://orcid.org/0009-0006-1415-8433
Hamed Sadeghi https://orcid.org/0000-0002-3453-9309

REFERENCES
1. Akbari Garakani, A., Tahajomi Banafshehvaragh, S., Saheb, S., & Sadeghi, H. (2025). Assessing the vulnerability of power transmission towers to land subsidence and forecasting future trends using multi-source datasets: insights from Moein Abad, Iran. *Innovative Infrastructure Solutions*, 10(4), pp.1-23. https://doi.org/10.1007/s41062-025-01958-3
2. Alonso, E. E., Vaunat, J., & Gens, A. (1999). Modelling the mechanical behaviour of expansive clays. *Engineering Geology*, 54(1-2), 173-183. https://doi.org/10.1016/S0013-7952(99)00079-4
3. Amarasiri, A.L., Kodikara, J.K., & Costa, S. (2011). Numerical modelling of desiccation cracking. *International Journal for Numerical and Analytical Methods in Geomechanics*, 35(1), pp.82-96. https://doi.org/10.1002/nag.894
4. Bernier, F., Li, X. L., & Bastiaens, W. (2011). Twenty-five years' geotechnical observation and testing in the Tertiary Boom Clay format. In *Stiff Sedimentary Clays: Genesis and Engineering Behaviour: Géotechnique Symposium* in Print 2007 (pp. 223-231). Thomas Telford Ltd. https://doi.org/10.1680/geot.2007.57.2.229
5. De Bruyn, D., & Labat, S. (2002). The second phase of ATLAS: the continuation of a running THM test in the HADES underground research facility at Mol. *Engineering Geology*, 64(2-3), 309-316. https://doi.org/10.1016/S0013-7952(01)00109-0
6. Delage, P., Sultan, N., & Cui, Y. J. (2000). On the thermal consolidation of Boom clay. *Canadian Geotechnical Journal*, 37(2), 343-354. https://doi.org/10.1139/t99-105
7. Feng, H., Xing, X., Su, L., Zhang, C., Wang, Y., Li, Y., & Wang, W. (2025). Insights into saline soil cracking subjected to drying-wetting cycles. *Acta Geophysica*, 73(1), 619-633. https://doi.org/10.1007/s11600-024-01375-7
8. Gambolati, G., & Teatini, P. (2015). Geomechanics of subsurface water withdrawal and injection. *Water Resources Research,* 51(6), 3922-3955. https://doi.org/10.1002/2014WR016841
9. Gao, H., An, R., Zhang, X., Wang, G., Liu, X., & Xu, Y. (2024). Dynamic evolution of desiccation cracks and their relationship with the hydraulic properties of expansive soil. *International Journal of Geomechanics*, 24(3), 04023299. https://doi.org/10.1061/IJGNAI.GMENG-9299
10. Gens, A., Vaunat, J., Garitte, B., & Wileveau, Y. (2007). In situ behaviour of a stiff layered clay subject to thermal loading: observations and interpretation. In *Stiff Sedimentary Clays: Genesis and Engineering Behaviour: Géotechnique Symposium in Print* 2007 (pp. 123-144). Thomas Telford Ltd. https://doi.org/10.1680/ssc.41080.0011

11. Ghandilou, M. J., Tourchi, S., & Sadeghi, H. (2023). Numerical investigation of cyclic wetting and drying of Boom clay based on the Barcelona Expansive Model. In *84th EAGE Annual Conference & Exhibition* (Vol. 2023, No. 1, pp. 1-5). European Association of Geoscientists & Engineers. https://doi.org/10.3997/2214-4609.202310400
12. Huang, Q., & Azam, S. (2023). Modeling of weather-induced volumetric changes in cracked expansive clays. *Geotechnical and Geological Engineering*, 41(2), 861-879. https://doi.org/10.1007/s10706-022-02310-7
13. Iran Meteorological Organization. (n.d.). *Data portal*. https://data.irimo.ir/
14. Jabbarzadeh, M. (2024). Thermo-hydro-mechanical modeling of heterogeneous subsidence in desiccation-cracked clayey strata under soil-atmosphere interactions. M.Sc. Thesis. Sharif University of Technology.
15. Jabbarzadeh, M., & Sadeghi, H. (2024). A novel analytical-statistical-numerical hybrid framework for investigating the thermo-hydro-mechanical behavior of heterogeneous subsidence phenomena, moisture and temperature variations in cracked soils under soil-atmosphere interaction. *Sharif Journal of Mechanical Engineering*. https://doi.org/10.24200/j40.2024.65047.1718
16. Jabbarzadeh, M., & Sadeghi, H. (2026). Multi-physical modeling of climate-driven elasto-plastic deformation, stress redistribution, and water potential in desiccation-cracked soils of arid regions. *Journal of Rock Mechanics and Geotechnical Engineering*, 18(1), 772-791. https://doi.org/10.1016/j.jrmge.2025.05.018
17. Jabbarzadeh, M., Sadeghi, H., Tourchi, S., & Darzi, A. G. (2024). Thermo-hydraulic analysis of desiccation cracked soil strata considering ground temperature and moisture dynamics under the influence of soil-atmosphere interactions. *Geomechanics for Energy and the Environment*, 38, 100558. https://doi.org/10.1016/j.gete.2024.100558
18. Liu, W., Song, X., Wan, S., Hu, X., & Zeng, X. (2025). Critical moisture content model and application to the formation of soil desiccation cracks. *Bulletin of Engineering Geology and the Environment*, 84(3), 147. https://doi.org/10.1007/s10064-025-04175-5
19. Mousavi, Z., & Jabbarzadeh, M. (2025). 3D DEM-based analysis of cylindrical rock specimen failure and micro-fracturing: impact of stiffness and tensile strength. *Discover Geoscience*, 3(1), 1-21. https://doi.org/10.1007/s44288-025-00126-5
20. Olivella, S., Carrera, J., Gens, A., & Alonso, E. E. (1994). Nonisothermal multiphase flow of brine and gas through saline media. *Transport in Porous Media*, 15, 271-293. https://doi.org/10.1007/BF00613282
21. Olivella, S., Gens, A., Carrera, J., & Alonso, E. E. (1996). Numerical formulation for a simulator (CODE_BRIGHT) for the coupled analysis of saline media. *Engineering Computations*, 13(7), 87-112. https://doi.org/10.1108/02644409610151575
22. Peron, H., Hueckel, T., Laloui, L., & Hu, L. (2009). Fundamentals of desiccation cracking of fine-grained soils: experimental characterisation and mechanisms identification. *Canadian Geotechnical Journal*, 46(10), pp.1177-1201. https://doi.org/10.1139/T09-054
23. Poulsen, T.G. (2022). Predicting evaporation from moist, cracked soil, based on near-surface wind speed, crack width and crack distance. *European Journal of Soil Science*, 73(1), p.e13215. https://doi.org/10.1111/ejss.13215
24. Poulsen, T.G., Cai, W., & Garg, A. (2020). Water evaporation from cracked soil under moist conditions as related to crack properties and near-surface wind speed. *European Journal of Soil Science*, 71(4), pp.627-640. https://doi.org/10.1111/ejss.12926
25. Qi, W., Zhang, Z. Y., Wang, C., Chen, Y., & Zhang, Z. M. (2020). Crack closure and flow regimes in cracked clay loam subjected to different irrigation methods. *Geoderma*, 358, 113978. https://doi.org/10.1016/j.geoderma.2019.113978
26. Sadeghi, H., Darzi, A. G., Voosoghi, B., Garakani, A. A., Ghorbani, Z., & Mojtahedi, S. F. F. (2023). Assessing the vulnerability of Iran to subsidence hazard using a hierarchical FUCOM-GIS framework. *Remote Sensing Applications: Society and Environment*, 31, 100989. https://doi.org/10.1016/j.rsase.2023.100989
27. Sadeghi, H., Jabbarzadeh, M., & Tourchi, S. (2024). Thermo-hydro-mechanical modelling of the heterogeneous subsidence and swelling in the desiccation cracked clayey strata. *Engineering Geology*, 343, 107798. https://doi.org/10.1016/j.enggeo.2024.107798
28. Sadeghi, H., Kolahdooz, A., & Ahmadi, M.M. (2022). Slope stability of an unsaturated embankment with and without natural pore water salinity subjected to rainfall infiltration. *Rock and Soil Mechanics*, 43(8), p.5. https://doi.org/10.16285/j.rsm.2021.00155
29. Tourchi, S., Jabbarzadeh, M., & Sadeghi, H. (2024). Thermo-hydro-mechanical analysis of soil strata suffered from desiccation cracking. In: *Geotechnical Engineering Challenges to Meet Current and Emerging Needs of Society* (pp. 1362-1367). CRC Press. https://doi.org/10.1201/9781003431749-249
30. Tourchi, S., Jabbarzadeh, M., Lavasan, A. A., Sadeghi, H., & Racek, O. (2024). Thermo-hydro-mechanical dynamics of a rock slope: Integrated field and numerical analysis at the Požáry test site in the Czech Republic. *Journal of Rock Mechanics and Geotechnical Engineering*. https://doi.org/10.1016/j.jrmge.2024.09.052

31. Tran, D. K., Ralaizafisoloarivony, N., Charlier, R., Mercatoris, B., Léonard, A., Toye, D., & Degré, A. (2019). Studying the effect of desiccation cracking on the evaporation process of a Luvisol–From a small-scale experimental and numerical approach. *Soil and Tillage Research*, 193, 142-152. https://doi.org/10.1016/j.still.2019.05.018
32. Valipour, M., Jabbarzadeh, M., Sadeghi, H., & Roghangar, K. (2024). Volumetric Behavior of a Soil Column Subjected to Freeze-Thaw Cycles Under Coupled Thermo-Hydro-Mechanical Conditions. *GeoMontréal* 2024. https://www.researchgate.net/publication/384431981
33. Van Genuchten, M. T. (1980). A closed-form equation for predicting the hydraulic conductivity of unsaturated soils. *Soil Science Society of America Journal*, 44(5), 892-898. https://doi.org/10.2136/sssaj1980.03615995004400050002x
34. Vicente-Serrano, S. M., N. G. Pricope, A. Toreti, E. Morán-Tejeda, J. Spinoni, A. Ocampo-Melgar, E. Archer, A. Diedhiou, T. Mesbahzadeh, N. H. Ravindranath, R. S. Pulwarty & S. Alibakhshi, (2024). *The Global Threat of Drying Lands: Regional and global aridity trends and future projections*. A Report of the Science-Policy Interface. United Nations Convention to Combat Desertification (UNCCD). Bonn, Germany.
35. Yan, C., & Wang, T. (2025). A 3D discrete model for soil desiccation cracking in consideration of moisture diffusion. *Journal of Rock Mechanics and Geotechnical Engineering*, 17(1), 614-635. https://doi.org/10.1016/j.jrmge.2023.12.024
36. Zeng, H., Tang, C. S., Zhu, C., Cheng, Q., Lin, Z. Z., & Shi, B. (2022). Investigating soil desiccation cracking using an infrared thermal imaging technique. *Water Resources Research*, 58(1), e2021WR030916. https://doi.org/10.1029/2021WR030916
37. Zeng, H., Tang, C. S., Zhu, C., Vahedifard, F., Cheng, Q., & Shi, B. (2022). Desiccation cracking of soil subjected to different environmental relative humidity conditions. *Engineering Geology*, 297, 106536. https://doi.org/10.1016/j.enggeo.2022.106536
38. Zeng, Z. J., Tang, C. S., Cheng, Q., An, N., Chen, X. Y., & Shi, B. (2023). A numerical model of water evaporation from cracked soil. *Computers and Geotechnics*, 162, 105641. https://doi.org/10.1016/j.compgeo.2023.105641
39. Zhou, H., Liu, H., Hu, D., Zhang, F., Yang, F., & Lu, J. (2016). Estimation of the effective thermal properties of cracked rocks. *European Journal of Environmental and Civil Engineering*, 20(8), 954-970. https://doi.org/10.1080/19648189.2015.1084386
40. Zhou, Z., Zhang, J., Ning, F., Luo, Y., Chong, L., & Sun, K. (2020). Large-scale test model of the progressive deformation and failure of cracked soil slopes. *Journal of Earth Science*, 31, 1097-1108.. https://doi.org/10.1007/s12583-020-1342-6
41. Zhuo, Z., Cai, W., Zhu, C., Tang, C. S., & Roksana, K. (2024). Morphology characterization of unsaturated soils under drying-wetting cycles: crack opening and closure. *Acta Geotechnica*, 1-20. https://doi.org/10.1007/s11440-024-02347-3